CHEMISTRY
A EUROPEAN JOURNAL

DOI: 10.1002/chem.200901333

VIP

Rhodamine Spiroamides for Multicolor Single-Molecule Switching Fluorescent Nanoscopy

Vladimir N. Belov,*[a] Mariano L. Bossi,[a] Jonas Fölling,[a] Vadim P. Boyarskiy,[a, b] and Stefan W. Hell*[a]

Dedicated to Professor Armin de Meijere on the occasion of his 70th birthday

Abstract: The design, synthesis, and evaluation of new rhodamine spiroamides are described. These molecules have applications in optical nanoscopy based on random switching of the fluorescent single molecules. The new markers may be used in (co)localization studies of various objects and their (mutual) positions and shape can be determined with a precision of a few tens of nanometers. Multicolor staining, good photoactivation, a large number of emitted photons, and selective chemical binding with amino or thiol groups were achieved due to the presence of various functional groups on the rhodamine spiroamides. Rigidized sulfonated xanthene fragment fused with six-membered rings, *N,N′*-bis(2,2,2-trifluoroethyl) groups, and a combination of additional double bonds and sulfonic acid groups with simple aliphatic spiroamide residue provide multicolor properties and improve performance of the rhodamine spiroamides in photoactivation and bioconjugation reactions. Having both essential parts of the photoswitchable assembly—the switching and the fluorescent (reporter) groups—combined in one chemical entity make this approach attractive for further development. A series of rhodamine spiroamides is presented along with characterizations of their most relevant properties for application as fluorescent probes in single-molecule switching and localization microscopy. Optical images with resolutions on the nanometer scale illustrate the potential of the labels in the colocalization of biological objects and the two-photon activation technique with optical sectioning.

Keywords: cage compounds · dyes/pigments · fluorescence · molecular switches · rhodamines

Introduction

The Abbe principle limits the optical resolution in far-field microscopy to about half the wavelength of the light used.[1] Several inventions in the last 10 to 15 years have demonstrated that the diffraction barrier may be broken by using reversible or irreversible photoswitching of the fluorescent probe between a dark and an emitting state.[2] The effective emitting volume, and thus the resolution, has been squeezed up to the size of a single (macro)molecule. These techniques can be subdivided according to the way the observed volume is reduced. Reversible saturable (switchable) optical fluorescence transitions (RESOLFT),[2a] the first family of techniques to overcome the Abbe limit, is based on a local squeezing of the effective fluorescent volume by means of illumination patterns that have one or more intensity zeros in the focal plane. This can be achieved using spotlike (focal) illumination scanned through the sample or by structured illumination. Recently, another family of techniques based on imaging stochastically switched single emitters has emerged, in which the position of the observed molecule is a priori unknown. The main advantage of this single-molecule switching microscopy (SMS; also known as photoactivation localization microscopy (PALM),[3] stochastical optical reconstruction microscopy (STORM),[4] or fPALM[5]) over the RESOLFT techniques is that it is not necessary to force the marker molecules to undergo many photoswitching cycles. However, SMS application requires samples with very low

[a] Dr. V. N. Belov, Dr. M. L. Bossi, Dr. J. Fölling, Dr. V. P. Boyarskiy, Prof. Dr. S. W. Hell
Department of NanoBiophotonics
Max Planck Institute for Biophysical Chemistry
Am Fassberg 11, 37077 Göttingen (Germany)
Fax: (+49) 551-201-2506
E-mail: vbelov@gwdg.de
shell@gwdg.de

[b] Dr. V. P. Boyarskiy
Permanent address: Chair of Physical Organic Chemistry
Chemistry Department, St. Petersburg State University
198504 St. Petersburg (Russia)

WILEY InterScience DISCOVER SOMETHING GREAT
© 2009 Wiley-VCH Verlag GmbH & Co. KGaA, Weinheim

background levels and, therefore, a high contrast between the molecular states of the markers used.

The working principle of the SMS approach consists of switching on and off a multitude of isolated markers, localizing them, and then reconstructing the image of the sample from their positions. The markers are imaged onto the camera of a wide-field microscope; each marker producing a diffraction-limited spot. The irradiation conditions are maintained in such a way that the number of molecules in the fluorescent state is low enough and their average distance is larger than the classical resolution. The center of the spot provides the position of the marker with an accuracy that ideally depends only on the number of collected photons, n, and on the full width at half maximum (FWHM) of the fluorescence spot, and is approximately given by $\mathrm{FWHM}/\sqrt{n}$.[6] Thus, provided that enough photons are collected from a single molecule, its position can be determined with an accuracy below the diffraction limit. After being imaged and localized, the markers must go back to a dark state (i.e., become bleached), so other markers can be switched on, localized, and switched off again. The process is repeated for a large set of markers and their positions are mapped to give an image with a resolution far better than the Abbe limit, ideally equal to the average localization accuracy of the individual markers. Besides the fluorescence switching, several requirements must be fulfilled for the markers to perform well in SMS. First, highly photostable dyes with large fluorescence quantum yields are required. In the fluorescent "on" state they should yield a large number of photons. Second, high contrast between the two states (fluorescent and dark) is necessary for measuring densely stained samples and allowing the reliable localization of a large number of markers. This ensures that in the dark state all markers produce a negligible contribution to the background when the switched-on molecules are imaged. Finally, the switching reactions should be easily controlled to keep the desired fraction of markers in the "on" state during the acquisition time.

Initially, SMS was realized by using photoactivable fluorescent proteins (PA-FPs)[3a] and activator–reporters sets of dyes composed of an Alexa Fluor (activator) and a cyanine dye (reporter; for example, Cy5).[4a,d] Both of them were performed in thin samples (cryosectioned) or in TIRF (total internal reflection fluorescence) geometries without axial resolution. The introduction of rhodamine spiroamides (RSAs) as photoactivable markers in SMS addressed the lack of axial resolution and provided optical sectioning by using two-photon activation (2PA). The photochromic reaction of RSA, reported in the 1970s by Knauer and Gleiter,[7] is presented in Scheme 1. The photoinduced ring-opening reaction generates the rhodamine chromophore, which typically absorbs in the green region and emits in the red (e.g., at $\lambda \approx 560$–580 nm for rhodamine B derivatives with $R_1 = R_2 = Et$). The closed spiro form is transparent across the whole visible range, providing a huge contrast between the signals of the two states. The open isomer returns thermally to the closed form (CF) with a characteristic lifetime of a few milliseconds in polar solvents[8] (longer in nonpolar solvents). Because SMS does not require a large number of cycles per marker to be performed (just one cycle is sufficient), the photobleaching and other secondary processes shown in Scheme 1 do not limit the use of RSAs in SMS. In fact, markers in the open form (OF) are bleached by a strong pulse of the same excitation laser after being imaged, to reduce imaging times.[9]

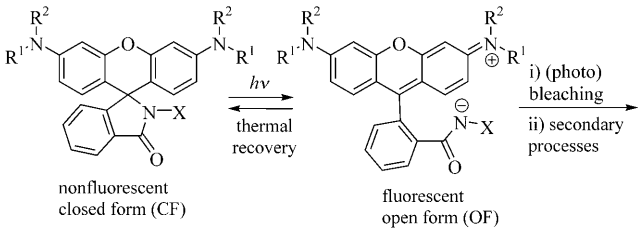

Scheme 1. Photochromic (caged) RSAs in the colorless CF and colored OF forms.

The first photochromic RSA used in SMS was aromatic spiroamide **1d** (Figure 1), derived from rhodamine B.[9] Highly photostable under single-molecule conditions, it allowed the detection of enough photons and provided an average localization precision of up to 10 nm. The usefulness of compound **1d** was demonstrated in inorganic materials (silica gel nanobeads) and in biological samples. Photoswitching between the isomers was realized by a one-photon activation process (1PA) at $\lambda = 375$ nm and a 2PA process at $\lambda = 747$ nm. The latter provided optical sectioning, allowing the measurement of samples several microns thick and a 3D reconstruction by imaging subdiffractionally resolved z stacks with ≈ 500 nm spacing. Combined with an asynchronous image acquisition protocol,[10] meaningful images were recorded in about 2–5 min. Rhodamine amide **1e**[11] was later introduced to improve the two-photon switching efficiency with continuous-wave laser sources, which also simplified the experimental setup.

Multicolor extensions of SMS by using PA-FPs,[3b] a combination of different activator–reporter systems,[4b,d] or mixtures of a PA-FP and Cy-5[12] have also been reported. In the last example, an activator was not used. The fluorescence of Cy-5 can be temporarily switched off by a strong laser light (ca. 10 kW cm^{-2}) of the same wavelength used for its excitation ($\lambda = 633$ nm),[13a] and this process can also be used without any activator for the acquisition of nanoscopic images.[13b] However, this switching process is sometimes difficult to control. The label may spontaneously go into the "on" state and it is highly sensitive to the (micro)environment and the presence of oxygen or triplet scavengers. Fluorescent proteins have the advantage of being genetically encodable, but they yield a low average number of photons. Activator–reporter systems are brighter but require special experimental conditions (e.g., oxygen-scavenging buffers or a triplet quencher at high concentration). Cyanine dyes (Cy3, Cy5, and Cy7) are used as reporters, and an adequate Alexa Fluor dye is typically selected as an activator.[4] Sec-

 © 2009 Wiley-VCH Verlag GmbH & Co. KGaA, Weinheim

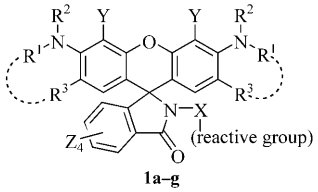

1a–g

a: R^1, R^3 = -$(CH_2)_3$-
R^2 = Z = H
Y = SO_3Na, X = CH_2CH_2COONa

b: R^1 = CH_2CF_3
R^2 = R^3 = Y = Z = H
X = Phth

c: R^1 = CH_2CF_3, R^2 = Et
R^3 = Y = Z = H,
X = Phth

d: R^1 = R^2 = Et
R^3 = Y = Z = H
X = Phth

e: R^1, R^3 = -CMe_2CH=C(Me)-
R^2 = Me, Y = Z = H
X = Phth

f: R^1, R^3 = R^2
Y = -$(CH_2)_3$-, Z = F
X = Phth

g: R^1, R^3 = -CMe_2CH=$C(CH_2SO_3H)$-
R^2 = Me, Y = Z = H
X = CH_2CH_2OH (alkylammonium salt)

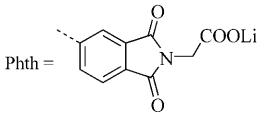

Figure 1. RSAs **1a–g** for multicolor single-molecule photoactivation experiments; approximate values for the fluorescence maxima of lithium salts in water or aqueous MeOH: **1a** $\lambda_{em} \approx 560$ nm, **1b** $\lambda_{em} \approx 530$ nm, **1c** $\lambda_{em} \approx 560$ nm, **1d** $\lambda_{em} \approx 590$ nm, **1e** $\lambda_{em} \approx 620$ nm, **1f** $\lambda_{em} \approx 630$ nm, **1g** $\lambda_{em} \approx 620$ nm. Stokes shifts for all compounds are ≈15–20 nm.

ondary antibodies have to be labeled with both the activator and the reporter in carefully selected proportions to optimize their distance and avoid the presence of more than one reporter molecule per antibody, which would result in a drastic reduction in the switching-off efficiency. Therefore, the photochromic RSA methodology seems to offer a viable alternative. This procedure is easier to control than the activator–reporter pair and PA-FP approaches. In fact, multicolor SMS based on two or more spectrally distinct photoactivable dyes (rhodamines) attached to different nanoparticles, antibodies, or "drug-like" molecules that "recognize" various bio-objects or receptors have already been proposed and implemented.[14]

Herein, we describe the design, synthesis, and evaluation of new fluorophores for SMS with nanoscopic resolution (Figure 1). The use of some of these new switchable fluorescent dyes as labels in the imaging of nanoparticles and (co)localization studies of various biological objects with resolutions of up to 10 nm has already been reported.[9,11,15] All of them may be activated in 1PA or 2PA processes with commercial lasers and provide multicolor staining, improved performance in aqueous media (**1a**), a high number of emitted photons, selective chemical binding with biomolecules (**1a**-$NHCH_2CH_2$-maleimide vs. NHS esters obtained with **1b–g**), and high photostabilities in both the CF and OF. New substituents at the nitrogen atoms and in the benzoic acid residue have been introduced. They predictably change the properties of the photoactivable assemblies.

Results and Discussion

Design and synthesis: The preparation of lithium salt **1d** and the active esters of the corresponding carboxylic acid have been previously reported.[9] They provided nanoscopic images of immunostained (in the tubuline network) whole fixed cells with the possibility of 2PA and optical sectioning. Screening of the amines allowed us to obtain a marker with the desired switching-on efficiency at $\lambda = 375$ nm. At this and longer wavelengths, conventional lenses have a high transmittance and inexpensive laser sources are available. It was found that an aromatic amine was necessary to provide an adequate activation rate and maintain a sufficient fraction of molecules per frame in the emitting state. An increase in the 2PA rate was achieved with the same 4-aminophthalimide derivative simply by changing from rhodamine B to rhodamine 590 (**1e**).[11] Though it is widely used in life science applications, the former is not an ideal fluorescent dye; its fluorescence quantum yield is fairly good ($\Phi_{fl} = 0.65$ in basic EtOH) but strongly depends on the temperature and solvent. Amides of rhodamine B absorb at about $\lambda = 565$ nm and emit at around $\lambda = 580$ nm (in the OF). Further optimization resulted in compounds **1a**, **1c**, and **1g**, which have been used for the realization of the multicolor far-field fluorescence nanoscopy with isolated detection of distinct molecular species,[15] but the principles of their design and preparation procedures have not yet been published. Here we fill this gap and describe the synthesis and properties of the whole series of RSAs that we have prepared for different SMS applications.

A spectral shift in the absorption and emission bands of a rhodamine is an easy and interesting option that may provide a "brighter" dye, more detectable photons (better localization precision), and another color, valuable for the colocalization studies and other applications in the future. We screened several amines and rhodamines before we developed compounds **1a–g** for multicolor single-molecule photoactivation and localization microscopy.[9,11,15] Rhodamines 6G and 110 could in principle afford a blue spectral shift (compared with rhodamine B), if the reactivity of the mono (e.g., in rhodamine 6G) or unsubstituted amino groups (e.g., in rhodamine 110) did not preclude the implementation of this plan. Binding with non-nucleophilic aromatic amines requires very strong activation of the sterically hindered carboxylic group of the rhodamine.[16] In practice, only acid chlorides were found to be reactive enough. Unfortunately, boiling of rhodamine 110 or rhodamine 19 (the free carboxylate of rhodamine 6G) with $POCl_3$ in dichloroethane did not produce a stable acid chloride but only a tar, probably

 © 2009 Wiley-VCH Verlag GmbH & Co. KGaA, Weinheim

due to self-condensation of the amino groups. Rhodamines B and 590 (**14**-H) have tertiary amino groups and their amidation is impossible. Therefore, they smoothly give the corresponding acid chlorides and then amides, even with relatively unreactive aromatic amines. To prevent an internal acylation, a new approach was required.

As a viable alternative to the sluggishly reacting aromatic amines, much more nucleophilic aliphatic amines may be used for amidation. However, the aromatic 4-amino-*N*-(methoxycarbonylmethyl)phthalimide (**18**) has some drawbacks: its incorporation reduces the water-solubility of the corresponding amides, and the phthalimide cycle is readily destroyed under basic conditions.[17]

We used a much more reactive methyl 3-aminopropionate, which amidated the water-soluble orange fluorescent dyes with a rigidized xanthene fragment (compound **2** in Scheme 2).[18] The colorless methyl ester **3**-OMe was formed in the presence of Et_3N and isolated from the reaction mixture by chromatography on SiO_2 with MeOH/diethyl ether (1:1) as the eluent. Interestingly, under these conditions amino sulfonic acid **3**-OMe was isolated as an inner salt (without Et_3N). Sodium salt **1a** can be efficiently photoactivated by irradiation at $\lambda = 375$ nm even though it has no extended conjugation in the amide part of the molecule. Fusion of the 3′,6′-diaminoxanthene fragment with two cyclohexane rings turned out to be sufficient for the photoactivation rate required for SMS, even in the absence of any aromatic amine residue. Surprisingly, sodium salt **1a** also absorbs in water with a maximum at $\lambda = 330$ nm ($\log\varepsilon \approx 4$), whereas the UV spectrum of reference compound **1d** has only a shoulder at $\lambda \approx 314$ nm with a similar absorbance.[19] Photoactivation of colorless sodium salt **1a** produces an orange fluorescent dye ($\lambda_{max} \approx 530$ nm, $\lambda_{em} \approx 550$ nm)[18] with an emission color that can be quite easily distinguished from that of rhodamine B amides ($\lambda_{em} \approx 570$ nm).[9] Alternatively, chemical "activation" is possible: passing an aqueous solution of **1a** through a cation-exchange resin in the H^+ form produced a highly colored solution of acid **3**-OH. Compound **1a**, however, could not be transformed into the stable amino reactive NHS ester under basic conditions because it acylates its own secondary amino groups, even at 0 °C. The unprotonated amino groups in **1a** and in the corresponding active esters are nucleophilic enough, even if they are somewhat sterically hindered by the sulfonic acid residues. *N*-(2-Aminoethyl)maleimide is much more reactive than the sterically hindered aromatic amino groups in **1a**. Therefore, we coupled **1a** with *N*-(2-aminoethyl)maleimide to give thiol reactive derivative **3**-$NHCH_2CH_2$-maleimide. The required compound was isolated in the OF as a red solid by preparative RP-HPLC (with 0.1 % v/v of trifluoroacetic acid in MeCN/water). It is stable in the absence of water and in the dark. Column chromatography on SiO_2 is accompanied by partial decomposition by water absorbed on the silica gel. Compound **3**-$NHCH_2CH_2$-maleimide may not only be used for the reaction with cysteine residues in proteins but also for binding with thiols, which appear after modification of the terminal amino groups of lysines with Traut's reagent.[15,20] Under slightly basic conditions (pH 7.5–8.5) it decolorizes and forms colorless bioconjugates.

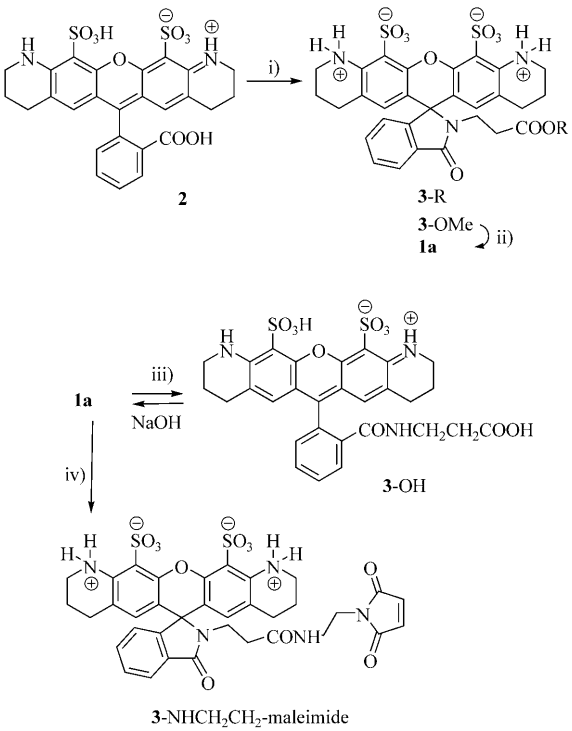

Scheme 2. Synthesis of primary aliphatic amides of sulfonated rhodamines with a rigidized xanthene fragment. Conditions: i) *N,N,N′,N′*-tetramethyl-*O*-(*N*-succinimidyl)uronium·BF_4^- (TSTU), Et_3N, DMF (*N,N*-dimethylformamide), RT, overnight; $HCl{\cdot}H_2NCH_2CH_2COOMe$, Et_3N, DMF, RT, overnight, 38–66 %; ii) aqueous NaOH (0.1–0.15 M), RT, 2 h, 100 %; iii) Amberlite IR-120 (H^+ form); iv) *N*-(2-aminoethyl)maleimide trifluoroacetate, *O*-(7-azabenzotriazol-1-yl)-*N,N,N′,N′*-tetramethyluronium·PF_6^- (HATU), DMF, RT, overnight, 26 %.

A further hypsochromic shift in the absorption and emission bands may be provided by rhodamine 110, which absorbs at around $\lambda = 490$ nm and emits at about $\lambda = 510$ nm. To prevent acylation of the unsubstituted amino groups in this fluorescent dye, a new protecting group that does not influence the spectra and allows the formation of the xanthene heterocycle from the corresponding aniline is required for the nitrogen atoms. The inductive effect of the CF_3CH_2 group is very similar to the inductive effect of the hydrogen atom. For example, 2,2,2-trifluoropropionic acid (CF_3CH_2COOH) is as strong as formic acid (HCOOH). Therefore, all rhodamine derivatives with 2,2,2-trifluoroethylated nitrogen atoms are expected to have the same absorption and emission spectra as the parent dyes. Moreover, the $NHCH_2CF_3$ groups in amino acid derivatives are known to be resistant to acylation (in the presence of "normal" primary amines).[21] Thus, this residue may also provide sufficient chemical protection for the amino group. The 2,2,2-trifluoroethyl group is easy to introduce (Scheme 3). Trifluoroacetylation of *m*-anisidine (**4**) and *N*-ethyl-3-methoxyaniline (**6**-Me) provides amides **5**-CF_3 and **8**, which may be reduced to **6**-CF_3 and **9**, respectively, by using BH_3·THF. The

 © 2009 Wiley-VCH Verlag GmbH & Co. KGaA, Weinheim

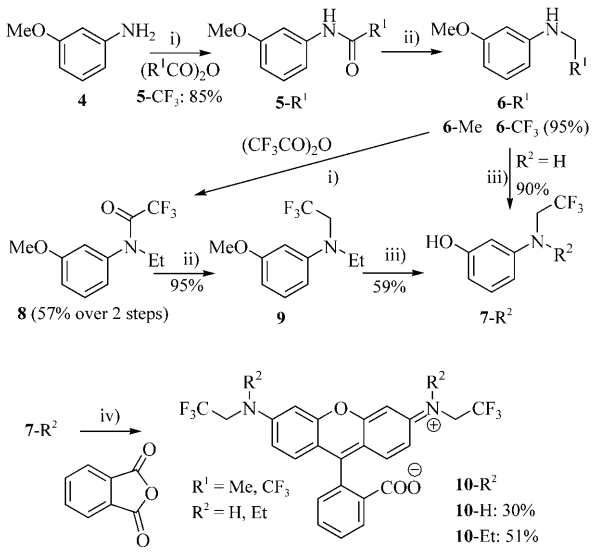

Scheme 3. Synthesis of rhodamines **10**-R^2 with *N*,*N*′-bis(2,2,2-trifluoroethyl) groups. Conditions: i) pyridine, CH_2Cl_2, RT, overnight; ii) BH_3·THF (1 M), THF, reflux, overnight; iii) 48% aqueous HBr, AcOH, reflux, 6 h; iv) 160 °C, 3 h, then portion 2 of **7**-R^2, 85% aqueous H_3PO_4, 160 °C, 3 h.

latter were demethylated, and phenols **7**-H and **7**-Et were condensed with phthalic anhydride to afford the required fluorescent rhodaminic dyes **10**-H and **10**-Et. These may be easily isolated from the reaction mixtures in gram quantities by crystallization, without using column chromatography. Gratifyingly, the excitation and emission spectra of xanthene dye **10**-H and rhodamine 110 were found to be very similar. Moreover, compound **10**-Et turned out to be a spectral analogue of rhodamine 6G with protected amino groups. Compound **10**-H is a red solid that exists in the OF as a zwitterion and is moderately soluble in unpolar solvents (e.g., $CHCl_3$). Substance **10**-Et is nearly colorless in the solid state. It readily dissolves in $CHCl_3$ and THF (but not in water) and its solutions are colorless. In the solid state and in nonpolar solvents it exists in a CF. The chemical shift of C9 in the xanthene fragment is diagnostically important; in the CF the ^{13}C NMR spectroscopic signal of the quaternary aliphatic spiro carbon atom is found at about $\delta = 84$ ppm and in the OF this signal shifts downfield and "disappears" in the densely populated region between $\delta = 110$ and 140 ppm. Transformation of the carboxylic groups in **10**-H and **10**-Et into the intensely colored acid chlorides can easily be performed by heating at reflux with $POCl_3$ in dichloroethane. Under these conditions, rhodamine **10**-H forms an insoluble intermediate that, however, further reacts as the corresponding acyl chloride. The amidation reactions (Scheme 5) will be discussed below.

Lithium salt **1e** can be photoactivated more easily than the similar rhodamine B derivative, **1d**, due to the presence of two additional double bonds; the resulting higher absorption at $\lambda = 375$ nm is assigned to the CF. Improved 1PA with $\lambda = 375$ nm light has been demonstrated for lithium salt **1e** itself (in a PVA matrix) and silica gel nanobeads stained with the NHS ester prepared from compound **1e**.[11] The ex-

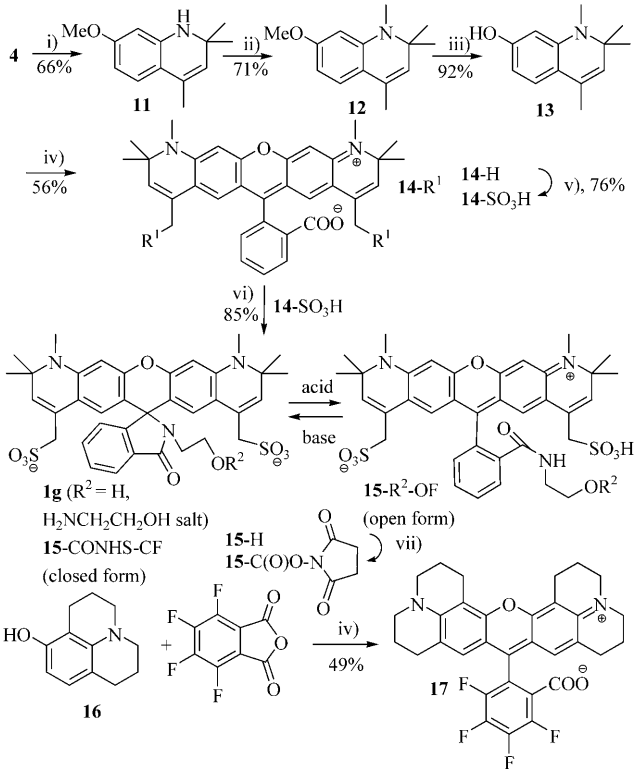

Scheme 4. Synthesis of rhodamines **1g** (**15**) and **17**, which absorb at $\lambda \approx 600$ nm and emit at $\lambda \approx 620$ nm. Conditions: i) acetone, $Y(OTf)_3$ (5 mol%), 24 h, RT; ii) MeI, Cs_2CO_3, DMF, 90 °C, 3 h; iii) 48% aqueous HBr, AcOH, reflux, 6 h; iv) *p*-TosOH, EtCOOH, 160 °C, 24 h; v) 96% H_2SO_4, 0 °C to RT, overnight; vi) $H_2NCH_2CH_2OH$; HATU, Et_3N, DMF, 40–50 °C, overnight; vii) di(*N*-succinimidyl)carbonate, Et_3N, MeCN, CH_2Cl_2, 50 °C, 2 h.

tended conjugation in compound **1e** also resulted in a better 2PA efficiency with respect to **1d**. This allowed the use of continuous-wave light sources in the red region of visible light for 2PA[11] instead of the more expensive pulsed sources necessary for 2PA-SMS with markers derived from **1d**. The absorption and emission spectra of compounds **1e** and **1g** (OF) are also redshifted to an extent of about 40 nm in comparison with the corresponding spectra of compound **1d** (OF) as a result of the extended conjugation. This allowed the use of both **1d** and **1e** in multicolor colocalization studies.[15] Unfortunately, the low water solubility of lithium salt **1e** and the active esters of the corresponding carboxylic acid preclude their use in biological applications. The presence of two additional double bonds in the six-membered rings fused with the xanthene core of compound **14**-H is advantageous. They provide the required absorption in the near-UV region, even without a heavy and rather nonpolar 4-aminophthalimide fragment as an additional chromophore.

Simple ω-amino acids—rather polar and water-soluble compounds—may be used as linkers instead of the 4-aminophthalimide residue. Further hydrophilization of dye **14**-H is provided by sulfonation with conc. H_2SO_4.[22] However, the carboxylic group in disulforhodamine **14**-SO_3H cannot be

 © 2009 Wiley-VCH Verlag GmbH & Co. KGaA, Weinheim

activated by heating with $POCl_3$ because this reagent readily transforms sulfonic acid residues into the corresponding sulfochlorides. Fortunately, selective activation of the carboxylate with HATU followed by coupling with aliphatic amines in the presence of sulfonic acid residues is possible. ω-Amino alcohols may be used instead of esters of the ω-amino acids. This modification shortens the reaction sequence because it requires commercially available reagents and omits the saponification of a methyl ester. NHS carbonates are known to be highly amino-reactive and their stability is sometimes even higher than that of NHS esters. Starting from 2-aminoethanol and sulforhodamine **14**-SO_3H, we synthesized compound **1g** (Scheme 4) and isolated it as a salt with an excess of 2-aminoethanol by using column chromatography on SiO_2. Before converting **1g** into NHS carbonate **15**-CONHS, the primary amine was removed by ion-exchange chromatography and the highly colored OF, disulfonic acid **15**-H-OF, was isolated. Complete conversion of **15**-H-OF into **15**-CONHS required a large excess of di(*N*-succinimidyl)carbonate and was achieved after several hours at about 50 °C in the presence of Et_3N. The pure final product, **15**-CONHS, was isolated in the OF as a dark blue solid by preparative RP-HPLC. It was stable for several weeks under anhydrous conditions in the dark at about −20 °C. It quickly decolorized in water under neutral or basic conditions. Interestingly, it took several tens of minutes after acidification for the blue color to reappear. To improve the photochemical stability of the red marker, we prepared rhodamine **17**, which absorbs and emits at practically the same wavelengths as **14**-R^1 (Scheme 4). It is an analogue of one of the most photostable fluorescent dyes, rhodamine 110 ($\lambda_{em} \approx 589$ in MeOH), with a perfluorinated benzoic acid ring. Electron-acceptor groups at C9 of the xanthene ring (opposite the oxygen atom) produce a bathochromic shift of both absorption and emission maxima, so that rhodamine **17** absorbs at about $\lambda = 595$ nm and emits at approximately $\lambda = 610$ nm. Compound **17** is very nonpolar and lipophilic, therefore, for better solubility in water and aqueous buffers in bioconjugation experiments, its spiroamides with a reactive group should contain hydrophilic residues.

Lipophilic rhodamines **10**, **14**, and **17** were treated with $POCl_3$ in boiling 1,2-dichloroethane and the corresponding acid chlorides were amidated with *N*-(methoxycarbonylmethyl)-4-aminophthalimide (**18**; Scheme 5). The cleavage of methyl esters and chemical activation of the aliphatic carboxy group was carried out as shown in Scheme 5. If a methyl ester was cleaved with LiI in boiling THF but not in ethyl acetate, the reaction was slower because of the lower boiling point of THF. However, ethyl acetate reacted with LiI and produced lithium acetate, so part of the reagent was lost. For the conjugation with biomolecules, lithium salts **1b–f** can be directly converted into corresponding NHS esters **20b–f** or, if higher solubility in water is desired, into the *N*-hydroxy(sulfosuccinimidyl) esters. These transformations and photoactivation parameters have been already reported for lithium salt **1d**,[9] which is also included in the following section for comparison.

Spectral properties: The spectral properties of the new switchable fluorescent dyes were studied to evaluate their applicability as molecular markers in SMS. The absorption and emission spectra of compounds **1a–g** were recorded in water. The effect of pH on the equilibrium between the open and closed isomers was also analyzed.

The absorption spectra of compounds **1a–g** are given in Figure 2. All the spectra show three main bands (with increasing intensities) at $\lambda = 310$–340 nm, $\lambda = 270$–290 nm, and $\lambda = 230$–265 nm. The positions of the first band (at longer wavelengths), which is the most appropriate band for activation purposes in microscopy, are listed in Table 1. Compounds **1a**, **1e**, and **1g** show a fairly good absorption at wavelengths of >350 nm. The other compounds displayed only a marginal absorption above $\lambda = 350$ nm, but it was enough for the low amount of activation needed for SMS. As a first approximation, we observed that modifications at the xanthene chromophore were more efficient at providing a bathochromic shift in the first band than changing the nitrogen substituent of the lactam (X in Figure 1 and Scheme 6). This conclusion became evident by comparing, for example, compound **1e** with compounds **1d** and **1g**. For recording the spectra of the open-ring isomers, irradiation of

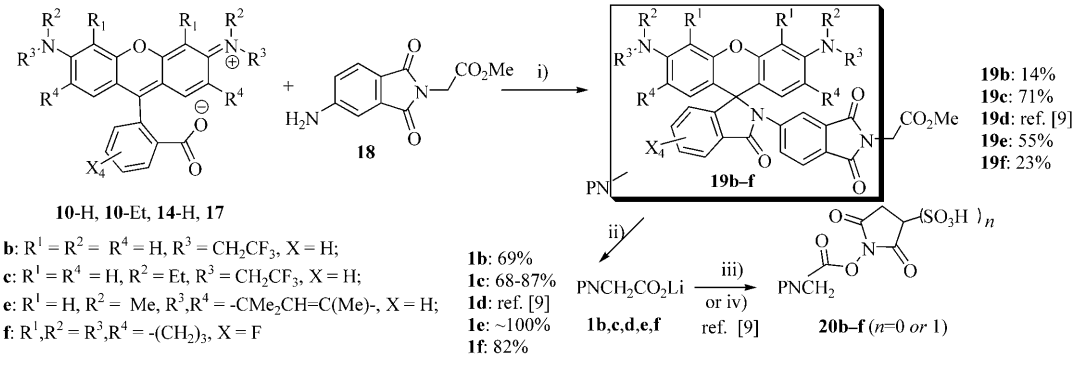

Scheme 5. Synthesis of methyl esters **19b–f** and the corresponding lithium salts **1b–f**. Conditions: i) $POCl_3$, 1,2-dichloroethane, reflux, 4 h, then **18**, MeCN, Et_3N, reflux, overnight; ii) LiI, EtOAc or THF, reflux, 2 or 4 d; iii) *N,N,N′,N′*-tetramethyl-*O*-(*N*-succinimidyl)uronium·BF_4^-, Et_3N, DMF, RT, overnight; iv) *N*-hydroxysulfosuccinimide, HATU, DMF, RT.

 © 2009 Wiley-VCH Verlag GmbH & Co. KGaA, Weinheim

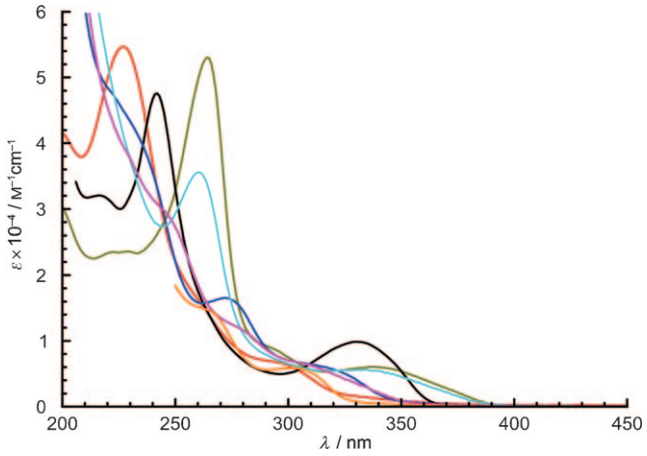

Figure 2. Absorption spectra of compounds **1a**–**g** in water. **1a**: ——; **1b**: ——; **1c**: ——; **1d**: ——; **1e**: ——; **1f**: ——; **1g**: ——.

Table 1. Spectral properties and K_a values of **1a**–**g** with mean numbers of emitted photons ($<n>$) after photoactivation of the CF and conversion to the OF.

	λ_{max}[a] [nm]			K_a	$<n>$[c]
	CF (abs)[b]	OF (abs)	OF (em)		
1a	331	537	555	2.2×10^{-5}	1600
1b	295	510	534	–[d]	1050
1c	301	536	557	–[d]	2350
1d	314	566	589	1.1×10^{-6}, 1.2×10^{-4}	1600
1e	338	596	618	3.2×10^{-6}	1350
1f	307	607	625	–[d]	1000
1g (**15**-H)	340	591	620	2.3×10^{-5}	850

[a] In water. [b] Maxima of the absorption band at the longest wavelength. [c] In PVA films. [d] Not measured.

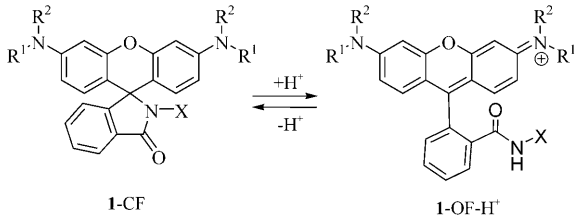

Scheme 6. Protonation-mediated ring-opening reaction of RSAs in water.

stirred solutions in water was attempted with a mercury lamp (2–6 mW at $\lambda = 365$ or 313 nm). In all cases, some fluorescence was observed under irradiation. However, thermal recovery (OF→CF) in water and polar solvents is known to be very fast (in the millisecond range)[8] and the spectra were difficult to measure. In less polar solvents (e.g., toluene), irradiation for about a minute under similar conditions (ca. 1–3 min) gave colored solutions that persisted for a few minutes depending on the compound and the solvent (data not shown). The spectra recorded under these conditions may be influenced by partial back isomerization to the CF during the data recording. Moreover, the spectral properties in nonpolar solvents differ considerably from those in the aqueous environment normally used in imaging experiments and as a mounting media (e.g., buffer solutions and Mowiol). Nevertheless, nonbuffered saturated aqueous solutions always contain small amounts of the OF due to the equilibrium presented in Scheme 6.

The emission spectra of the forms (OF-H$^+$) are presented in Figure 3, and the corresponding absorption maxima are listed in Table 1. The typical spectral features of the *N*-substituted rhodamine amides were observed, with yellow to red emission colors. This group of compounds comprises a tool-box from which up to four markers for multicolor experiments can be chosen.

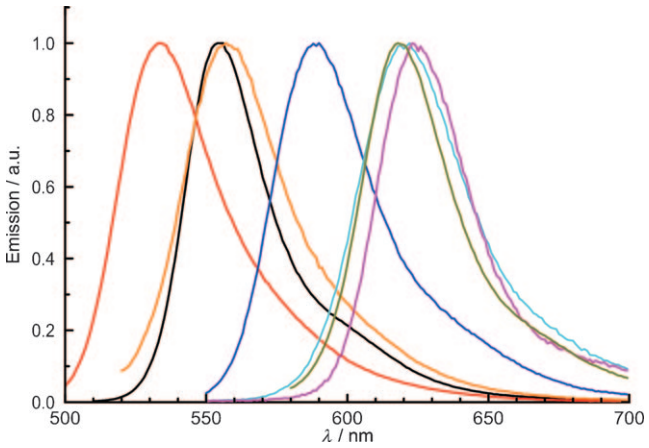

Figure 3. Emission spectra of the OFs (**1**-OF-H$^+$ in Scheme 6) of compounds **1a**–**g** in aqueous solutions: **1a**: ——; **1b**: ——; **1c**: ——; **1d**: ——; **1e**: ——; **1f**: ——; **1g**: ——.

The equilibrium presented in Scheme 6 was further studied in aqueous buffers in at pH values ranging from 2 to 12 (except for compounds **1b**, **1c**, and **1f**, due to their low solubility). The changes in absorption observed for compound **1g** on decreasing the pH value are presented in Figure 4A. At least three clear isobestic points confirm that only two species are present in the studied pH range. Similar effects were observed for compounds **1a** and **1e**.

Speciation diagrams for these three compounds are presented in Figure 4B and the calculated equilibrium constants are listed in Table 1. The proportion of the colored form (OF-H$^+$) was calculated from the absorption of the red band (see Table 1). The fluorescence lifetimes measured for the emitting species were in the range of 3 to 4 ns, and were similar to those of the unsubstituted parent rhodamines with free carboxylic groups. Moreover, the lifetimes did not depend on the pH value (in the studied range).

The acid-catalyzed ring-opening reaction in Scheme 6 competes with the light-induced reaction and, therefore, should be avoided when using these dyes as probes in single-molecule localization studies. The useful pH range can be estimated from the calculated acidity constants given in Table 1. All the compounds presented here can be used

 © 2009 Wiley-VCH Verlag GmbH & Co. KGaA, Weinheim

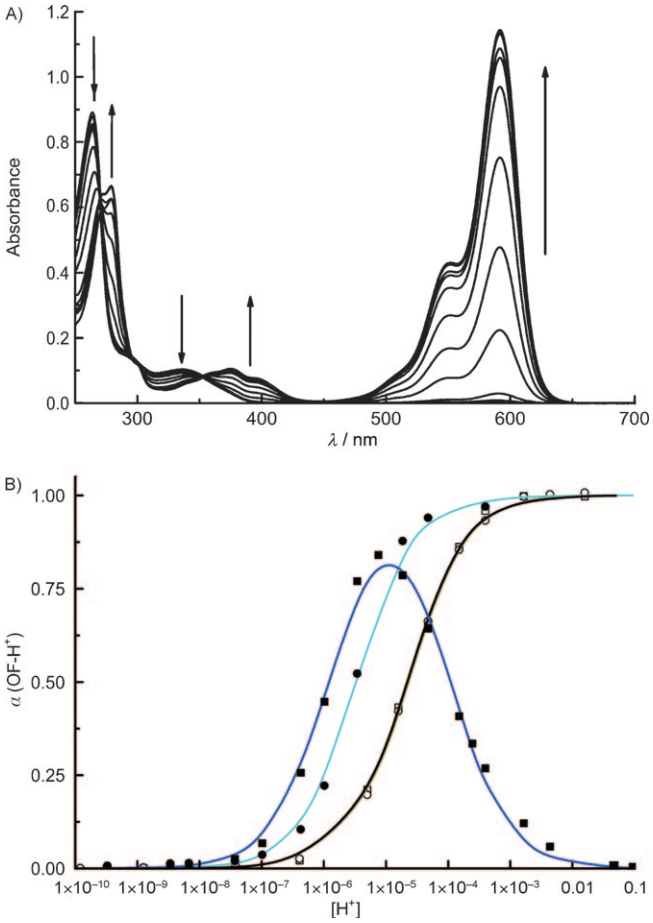

Figure 4. A) Effect of pH on the equilibrium shown in Scheme 6 for compound **1g**. The arrows display the direction of the changes as the proton concentration was increased (the pH was decreased from 12 to 2). B) pH speciation diagram for the colored forms of compound **1a** (□, ——), **1d** (■, ——), **1e** (●, ——), and **1g** (○, ——). The symbols correspond to measured data and the lines are best fits obtained by considering one (compound **1e**) or two equilibrium constants (compounds **1a**, **1d** and **1g**).

as probes at biologically relevant pH values (6.5–8.0). Compounds **1a** and **1g** may be also used at pH > 5.5. Compound **1d** also decolorizes in acidic solutions; probably due to protonation of the freely rotating *N*,*N*-diethyl amino group(s). In this case, alkyl residues increase the basicity of the nitrogen atoms to higher extent than other substituents in compounds **1a**, **e**, and **g** with a rigidized xanthene fragment.[23] The data shown in Figure 4 demonstrate another potential application for the compounds **1a**, **1d**, **1e**, and **1g**; they may serve as fluorescent pH indicators for the pH range of 3 to 7, depending on the dye. Moreover, the color of the indicator and, to some extent, the transition pH range can be independently tuned by selecting the rhodamine (R^1 and R^2) and the substituting amine (X).

Single-molecule behavior was studied in PVA films with the aim of obtaining the average number of photons that can be detected per molecule in the OF. This value is very important because it determines the resolution that can be achieved when the dyes are used as probes in SMS. The number of photons depends on the environment, therefore, PVA was selected because it is commonly used as a mounting media in imaging experiments and, unlike solutions (e.g., buffer solutions), there is no diffusion of the molecules during the acquisition of a frame. Because the value may also depend on the pH, the films for SM experiments were spin coated from mixtures of the corresponding dye and PVA in water-buffered solutions at pH 7.4.

Samples containing different dyes were exposed to low light intensities at $\lambda = 375$ nm in a wide-field microscope to ensure an appropriate amount of molecules in the OF. In general, an average of about 15 molecules per frame was used. A larger number of switching-on events is undesirable because it could result in two or more molecules being in the emitting state at a distance closer than the resolution of the microscope. Switched-on molecules were recorded by using an EM-CCD camera with a frame rate of 10 ms, and the number of photons detected per event was calculated. Figure 5 shows two examples of the histograms obtained

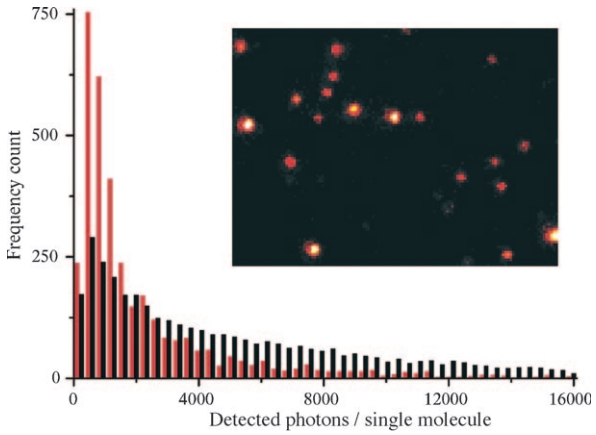

Figure 5. Histograms of the number of photons per single-molecule event for compound **1c** (black bars) and compound **1f** (red bars). The inset shows a typical frame from the CCD camera, from which single-molecule events were localized.

from a large number of single-molecule events (> 20 000), to ensure the statistic relevance of the data. The threshold to reject dim events was set to 80 photons; events yielding over 8000 photons were also neglected because at those levels the response of the camera is nonlinear at the gain factors used. The average values extracted from the histograms for all dyes are listed in Table 1. All the compounds are extremely bright and, calculated from the number of detected photons, theoretical localizations accuracies of single-molecule events are expected to be below 15 nm for all the dyes reported in Table 1. It should be noted that these values are environment dependent, and therefore may differ slightly in other applications or immersion media used for the measurements. An example of a CCD camera frame is presented in Figure 5, inset; the high signal-to-noise ratio demonstrates the excellent prospect of using RSAs for single-molecule applications. Based on the observed switching-on processes and the excellent brightness of all the dyes

 © 2009 Wiley-VCH Verlag GmbH & Co. KGaA, Weinheim

presented herein, it can be concluded that they are all promising as probes for SMS. The average number of photons detected per single-molecule event anticipates localization accuracies and, therefore, an achievable spatial resolution in the order of 10 to 15 nm for all measured compounds.

Fluorescence nanoscopy at the biomolecular level: Immunostaining is one of the most widespread procedures to deliver the required markers to the desired target (an organelle, a biomolecule, etc.) with high specificity and selectivity. Perhaps cellular biology is the most promising application field for RSAs as markers in fluorescence nanoscopy. Reactive analogues of the dyes are necessary to specifically stain the samples to be imaged. The amino-reactive NHS esters are the simplest choice and were selected whenever possible. Sometimes thiol reactive analogues were used to label secondary antibodies according to standard or new protocols.[15] For compounds **3**-$NHCH_2CH_2$-maleimide,[15] **15**-CONHS,[15] **20c**,[15] **20d**,[9,15] and **20e**,[11] we were successful and high-resolution images were obtained. In case of sodium salt **1a**, the corresponding NHS ester probably reacts with amine groups of the chromophore to form insoluble oligomeric or polymeric condensation products. In this case, a thiol-reactive derivative, **3**-$NHCH_2CH_2$-maleimide, was successfully used for labeling antibodies modified with Traut's reagent (2-iminothiolane). The standard protocol[24] was modified. The sheep anti-mouse IgG antibody was degassed and incubated with a ten-fold excess of Traut's reagent under nitrogen. Terminal amino groups of lysine residues ($H_2N(CH_2)_4$) were transformed into $HS(CH_2)_3C(=NH)NH(CH_2)_4$ groups and then thiol groups (and probably 2-iminothiolane) directly reacted with **3**-$NHCH_2CH_2$-maleimide, which was used in an equal amount with Traut's reagent. Intermediate purification of the thiolated antibodies[24] was not performed because it could have caused oxidation of thiol groups and formation of the corresponding disulfides. Finally, gel filtration through Sephadex G-25 (with standard phosphate-buffered saline) gave the labeled protein purified from low-molecular-weight compounds.

Lipophilic NHS esters **20b–f** (Scheme 5; $n=0$) are not soluble in water and under standard reaction conditions they provide low degrees of labeling. Increasing the amount of dye per antibody or the content of DMF in the aqueous buffer (up to 5% v/v) did not improve the degree of labeling. However, they were very efficient and gave excellent images in other applications in which organic solvents can be used in the labeling process. For example, NHS ester **20c** reacted with 3-aminopropyl triethoxysilane in DMF and was incorporated into silica nanobeads.[15,25]

After photoactivation of spiroamides **1g** (**15**-CONHS) with UV light ($\lambda=375$ nm) followed by excitation by green light ($\lambda=530$ nm), fluorescence with $\lambda_{max}\approx620$ nm was detected. After a large number of activation–excitation cycles, or prolonged irradiation with UV light ($\lambda=375$ nm), a blue-shift of the emission maximum to $\lambda\approx580$–590 nm was observed. This behavior may be explained by the (stepwise) "disappearance" of the two additional double bonds in compounds **14** and **1g** (**15**). They may easily oxidize, and irradiation in the presence of atmospheric oxygen and a dye that generates singlet oxygen may lead to an oxirane (which finally gives ring-opening products with a simple C–C bond instead of a double bond). This drawback caused time-dependent channel cross-talk, that is, a false assignment of detected single molecules in multicolor imaging.[15]

Violet or UV light ($\lambda=375$ nm), which is used for photoactivation, may cause cell damage and lead to autofluorescence, whereas red light minimizes these effects. Irradiation of RSAs **20b–f** with very strong red light also initiates a ring-opening reaction and produces fluorescent species in the course of the 2PA process.[9,11] The most important difference between 1PA and 2PA processes is that 2PA is only effective in a thin plane,[26] which allows optical sectioning. To demonstrate the applicability of 2PA with axial sectioning in cell biology, we imaged lamin proteins in the nucleus of a human glioma cell specifically labeled with secondary antibodies stained with *N*-hydroxysulfosuccinimidyl ester **20d** ($n=1$). Figure 6 shows a 3D reconstruction of nuclear lamina by combining nine images recorded at different z positions with a typical separation of 600 nm between slices. The "tubing" and folding inside the cell nucleus is distinctly seen in the series of pictures. This kind of tube-like connections is characteristic of the lamin skeleton of a nucleus. A good tangential resolution was achieved in this thick sample (>6 μm), demonstrating the feasibility of imaging in a whole (fixed) cell with no need for (cryo)sectioning.

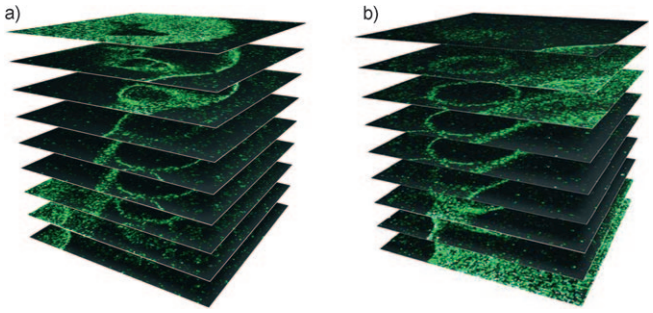

Figure 6. Optical sections of lamin proteins in the nucleus of a U373MG cell imaged by using 2PA with $\lambda=747$ nm light; field of view: 12.5 × 12.5 μm; pixel size: 30 nm; distance between z stacks ≈600 nm. Nuclear lamina of whole fixed human glioma cells, U373M, were stained with antilamin A mouse IgG as a primary antibody and sheep anti-mouse IgG labeled with *N*-hydroxysulfosuccinimidyl ester **20d** ($n=1$) as a secondary antibody.

Figure 7A shows a two-color high-resolution image of a PtK2 cell immunostained with compounds **20d** and **20e** ($n=1$) in the tubulin filaments and clatrin vesicles, respectively. The excellent brightness of the SRA dyes allows the application of a marker separation technique through a combination of single-molecule spectroscopy and microscopy[14,15] that provides an improved color separation (i.e., reduces false marker assignment) with respect to the conventional ensemble techniques normally used (for example, in confocal microscopy). Features beyond the classical resolution are

 © 2009 Wiley-VCH Verlag GmbH & Co. KGaA, Weinheim

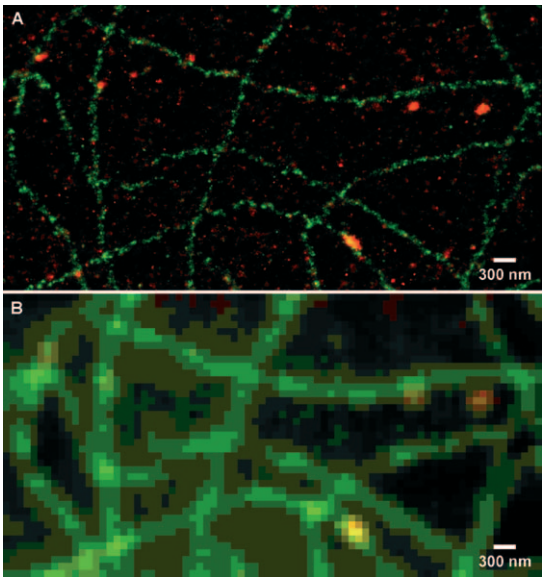

Figure 7. A) Two-color high-resolution SMS image of PtK2 cells with tubulin and clatrin structures immunostained by using compounds **20d** and **20e** ($n=1$), respectively. B) The same conventional wide-field image obtained by adding the individual single-molecule events.

clearly revealed in Figure 7A, reflecting the possibility of resolving objects that are blurred in a conventional microscope by employing the probes presented herein. Figure 7B shows the corresponding conventional wide-field image, which, apart from lower resolution, also shows worse color separation. Figure 7 demonstrates the applicability and prospective use of the RSAs for multicolor applications, such as colocalization of custom-stained objects or structures.

Conclusions

Having both essential parts of a dye (the activator (spiroamide) and the reporter (xanthene) groups) combined in one chemical entity allows tedious double staining procedures, which have been reported for the related STORM methodology,[4] to be avoided. New RSAs decorated with a reactive group may be used for bioconjugation and even help to overcome some drawbacks of large fluorescent proteins that may interfere with the physiological role of the studied protein after fusion and are known to be modestly photostable. In most cases (e.g., for the switchable fluorescent protein RSFP rsFastLime),[10] the reported average number of detected photons per single-molecule burst is about an order of magnitude lower than the typical values of 1400–2700 photons reported for RSAs.[15] Moreover, chemical linking of the photochromic rhodamines with FlAsH (ReAsH) or benzyl purines (pyrimidines) that recognize very small tetracysteine motifs or SNAP tags, respectively, may help to overcome drawbacks intrinsic to the PALM imaging of big fused PA-FPs or clusters of antibodies. Other photoactivable (caged) fluorophores, including those that can penetrate the plasma membrane and the intact cell wall (e.g., *N,N,N′,N′*-tetramethylrhodamine), are of particular interest. It is better to avoid the bulky aromatic amines that have been used to shift the absorption band edge to the near-UV region because they increase molecular masses and lipophilicity and reduce water solubility. New chromophores that provide highly efficient photoactivation, good solubility in water, "atom economy" (absence of unnecessary structural elements), high fluorescence quantum yields, and an appropriate reactive group (recognition site) are going to be developed. To keep the marker molecule small enough to penetrate through the walls of living cells, new types of photochemically active groups have to be introduced. In addition, the corresponding NHS ester can probably be prepared from OF **3**-OH, in which the amino groups are protected by protonation.

Very recently, a simple and yet very powerful super-resolution technique emerged. It is based on ground-state depletion followed by return of the individual molecules (GSDIM) to the ground state (S_0). This method uses commercially available fluorescent dyes and provides an optical resolution of $\lambda \approx 30$ nm.[27] However, it requires higher light intensities (which transfer nearly all dye molecules to a dark state) and, therefore, 2PA is more difficult. Thus, photoactivation of RSAs is a viable alternative to GSDIM, especially when imaging with optical sectioning is required.

Experimental Section

General remarks: UV/Vis absorption spectra were recorded by using a Varian Cary 4000 UV/Vis spectrophotometer and fluorescence spectra were recorded by using a Varian Cary Eclipse fluorescence spectrophotometer. Closed quartz cuvettes with a 1 cm path length were used in all experiments. All reactions were carried out with magnetic stirring in Schlenk flasks equipped with septa or reflux condensers with bubble-counters under argon or nitrogen (supplied by using a standard manifold with vacuum and argon lines). NMR spectra were recorded at 25 °C by using Varian MERCURY 300 (300 (^{1}H) and 75.5 MHz (^{13}C, APT)), Bruker AM 250 (250 (^{1}H) and 62.9 MHz (^{13}C, DEPT), INOVA-500 (125.7 MHz (^{13}C)) and INOVA-600 (600 MHz (^{1}H)) spectrometers. All spectra are referenced to tetramethylsilane as the internal standard ($\delta=0$ ppm) by using the signals of the residual protons of $CHCl_3$ (7.26 ppm) in $CDCl_3$, CHD_2OD (3.31 ppm) in CD_3OD, HOD (4.79 ppm) in D_2O, [D_5]acetone (2.04 ppm) in [D_6]acetone, or [D_5]DMSO (2.50 ppm) in [D_6]DMSO. Multiplicities of signals are described as follows: s = singlet, br = broad, d = doublet, t = triplet, q = quartet, quint = quintet, m = multiplet, m_c = centrosymmetrical multiplet. Coupling constants (J) are given in Hz. Multiplicities in the ^{13}C NMR spectra were determined by APT (attached proton test) measurements. Low-resolution mass spectra (ESI) were obtained by using an LCQ spectrometer. High-resolution mass spectra (ESI-HRMS) were obtained by using an APEX IV spectrometer (Bruker). HPLC system (Knauer): Smartline pump 1000 (2×), UV detector 2500, column thermostat 4000 (25 °C), mixing chamber, injection valve with 20 and 100 μL loops for the analytical and preparative columns, respectively; 6-port-3-channel switching valve; analytical column: Eurospher-100 C18, 5 μm, 250×4 mm, 1 mL min^{-1}; preparative column: Eurospher-100-5 C18, 5 μm, 250×8 mm, 4 mL min^{-1}; solvent A: water + 0.1 % v/v trifluoroacetic acid (TFA); solvent B: MeCN + 0.1 % v/v TFA. Analytical TLC was performed on MERCK ready-to-use plates with silica gel 60 (F254). Column chromatography: MERCK silica gel 60, 0.04–0.063 mm or Polygoprep 60-50 C18 (Macherey–Nagel). Amberlite IR-120 (H^+ form, VWR) was used as an ion-exchange resin. Elemental analyses were carried out at Mikroanalytisches Laboratorium des Insti-

 © 2009 Wiley-VCH Verlag GmbH & Co. KGaA, Weinheim

tuts für Organische und Biomolekulare Chemie der Georg-August-Universität, Göttingen. Organic solutions were dried over $MgSO_4$ or Na_2SO_4. Lithium salts **1b–f** were converted into the NHS esters **20b–f** according to a previously described procedure.[9]

Compound 3-OMe: Rhodamine **2** (0.29 g, 0.51 mmol) was suspended in DMF (9.5 mL) and TSTU (0.36 g, 1.2 mmol) was added in one portion, followed by Et_3N (0.5 mL, 3.5 mmol). The solution was stirred at RT for 20 h and then added to a solution of $HCl{\cdot}H_2NCH_2CH_2COOMe$ (0.56 g, 4.0 mmol) and Et_3N (1 mL, 7 mmol) in DMF (10 mL). After stirring for 3 d at RT, the DMF and excess Et_3N were removed under vacuum (ca. 1 mbar) and cold MeOH (6 mL) was added to the residue. After stirring at 0 °C for 1 h, the precipitate was separated, washed with cold MeOH (1 mL), and dissolved in MeOH (ca. 100 mL). This solution was diluted with diethyl ether and immediately filtered through SiO_2 (50 g). The title compound was eluted with MeOH/diethyl ether (1:1) and isolated as a light violet powder (128 mg, 38 %). M.p. >250 °C; ^{1}H NMR (600 MHz, [D$_6$]DMSO): δ = 1.64 (m, 4H), 2.26 (t, ^3J(H,H) = 7.6 Hz, 2H), 2.40 (A part of ABXY system, 2H), 2.50 (B part of ABXY system, J_{AB} = 12 Hz), 3.24 (m, 6H), 3.50 (s, 2H), 6.01 (s, 2H), 6.98 (d, ^3J(H,H) = 7.5 Hz, 2H), 6.98 (d, ^3J(H,H) = 7.5 Hz, 2H), 7.46 (t, ^3J(H,H) = 6.9 Hz, 2H), 7.52 (t, ^3J(H,H) = 6.9 Hz, 2H), 8.13 ppm (brs, 2H); ESI-MS (positive mode): *m/z*: 722 (58) $[M-2H+3Na]^+$, 732 (100) $[M-H+2K]^+$, 747.5 (79); ESI-MS (negative mode): *m/z*: 654 (46) $[M-H]^-$, 676 (100) $[M-2H+Na]^-$; HRMS: *m/z* calcd for $C_{30}H_{29}N_3O_{10}S_2$: 656.13671; found: 656.13633 $[M+H]$.

Compound 1a: Methyl ester **3**-OMe (115 mg, 0.175 mmol) was suspended in water (5 mL) at 0 °C and aqueous NaOH (1 M; 0.7 mL) was added dropwise. After stirring for 2 h at RT, the colorless solution became clear and HPLC indicated full conversion of **3**-OMe (t_R = 9.1 min) into **1a** (t_R = 7.1 min; eluent: A/B 80:20–50:50 in 25 min, 254 nm). ^{1}H NMR (300 MHz, D_2O): δ = 1.78 (m, 4H), 2.11 (m, 2H), 2.40–2.49 (m, 2H), 2.53–2.63 (m, 2H), 3.34 (m, 4H), 3.45 (m, 2H), 6.26 (s, 2H), 7.20 (m, 1H), 7.64 (m, 2H), 7.94 ppm (m, 1H); ESI-MS (positive mode) for $C_{29}H_{24}Na_3N_3O_{10}S_2$: *m/z*: 686 (72) $[M-Na+2H]^+$, 708 (100) $[M+H]^+$, 733.5 (29); ESI-MS (negative mode) for $C_{29}H_{24}Na_3N_3O_{10}S_2$: *m/z*: 640 (38) $[M-3Na+2H]^-$, 662 (100) $[M-2Na+H]^-$.

Compound 3-OH: Ion-exchange resin was washed with methanol, water, aqueous HCl (1 M) and again with water, until the pH value reached 4–5. Sodium salt **1a** (50 mg of freeze-dried solid with ca. 5 % (w/w) NaOH) was dissolved in water (0.5 mL) and passed slowly through the cation exchanger (ca. 5 mL). Washing it with water (10 mL) produced a strongly red colored solution that was lyophilized to acid **3**-OH (34 mg). ^{1}H NMR (300 MHz, D_2O): δ = 1.91 (m, 4H), 2.28 (t, ^3J(H,H) = 6.0 Hz, 2H), 2.71 (m, 4H), 3.33 (t, ^3J(H,H) = 5.9 Hz, 2H), 3.61 (m, 4H), 6.90 (s, 2H), 7.39 (m, 1H), 7.76 ppm (m, 3H); ^{13}C NMR (125.7 MHz, D_2O, MeOH 49.9 ppm): δ = 19.8 (2×CH_2), 28.3 (2×CH_2), 33.9 (CH_2), 36.1 (CH_2), 43.0 (2×CH_2), 111.9 (C), 113.5 (C), 126.6 (C), 128.5 (CH), 130.4 (CH), 131.3 (CH), 131.5 (CH), 131.8 (C), 131.9 (CH), 136.7 (C), 153.0 (C), 155.1 (C), 155.9 (C), 171.3 (CO), 176.1 ppm (CO); ESI-MS (positive mode): *m/z*: 686 (66) $[M-H+2Na]^+$, 708 (100) $[M-2H+3Na]^+$, 733.6 (25); ESI-MS (negative mode): *m/z*: 640 (100) $[M-H]^-$, 662 (98) $[M-2H+Na]^-$. In aqueous solutions at RT, **3**-H was found to slowly lose its sulfonic acid residues. Decomposition was complete in several months.

Compound 3-NHCH$_2$CH$_2$-maleimide: A mixture of sodium salt **1a** (21 mg, 30 μmol) and NaOH (8 mg, 200 μmol) was suspended in DMF (5 mL) and *N*-(2-aminoethyl)maleimide trifluoroacetate (39 mg, 153 μmol) was added, followed by HATU (27 mg, 71 μmol) to give a clear yellow solution with weak fluorescence, which was stirred overnight at RT. The solvent was evaporated in vacuo (1 mbar) and the glassy residue was separated on SiO_2 (25 g) to give the photoactive substance (R_f = 0.8; eluent MeOH/$CHCl_3$ 3:1) as a red foam (10 mg). The title compound (t_R = 8.8 min) was finally purified from the impurity (t_R = 10.5 min) by using HPLC (eluent: A/B 80:20–50:50 in 25 min, 254 nm) and isolated as red solid after lyophilization (6 mg, 26 % OF due to the presence of trifluoroacetic acid in the eluent). ^{1}H NMR (600 MHz, D_2O): δ = 1.93 (quint, ^3J(H,H) = 6.0 Hz, 4H), 2.09 (t, ^3J(H,H) = 7.0 Hz, 2H), 2.76 (m, 4H), 3.33 (t, ^3J(H,H) = 6.7 Hz, 2H), 3.32 (m, 2H), 3.63 (m, 6H), 6.87 (s, 2H), 6.97 (s, 2H), 7.48 (m, 1H), 7.83 ppm (m, 3H); ESI-MS (negative mode): *m/z*: 762 (100) $[M-H]^-$, 784 (44) $[M-2H+Na]^-$; HRMS: *m/z* calcd for $C_{35}H_{33}N_5O_{11}S_2$: 656.16907, 656.15102; found: 764.16883 $[M+H]$, 786.15082 $[M+Na]$.

General method for the preparation of *N*-acyl-*m*-methoxyanilines 5-Me, 5-CF$_3$, and 8: *m*-Anisidine **4** or *N*-ethyl-*m*-anisidine (**6**-Me; 0.10 mmol) and dry pyridine (0.12 mol) were dissolved in dry CH_2Cl_2 (200 mL) and cooled to 0 °C. Acetic or trifluoroacetic anhydride (0.12 mol) in CH_2Cl_2 (50 mL) was then added dropwise with stirring. The mixture was stirred overnight at RT and then washed with cold water (3×100 mL), aqueous HCl (1 M, 100 mL), and saturated aqueous $NaHCO_3$ (100 mL). After drying, the solvent was evaporated in vacuo and the crystalline residue was, as a rule, used in the next reduction step without further purification (yields 85–100 %). Compound **9** was purified by using chromatography on SiO_2 with hexane/EtOAc (8:1) to remove the impurity with a lower R_f (yield 74 %).

General method for the reduction of amides 5-Me, 5-CF$_3$, and 8; synthesis of amines 6-Me, 6-CF$_3$ and 9: A solution of BH_3 in THF (1 M; 160 mL) at 0 °C was added to amide **5**-R^1 or **8** (80 mmol) in dry THF (50 mL), and the mixture was heated at reflux overnight before being cooled to 0 °C. Excess BH_3 was carefully neutralized by adding MeOH (20 mL), and then aqueous NaOH (1 M) was added. After stirring at RT for 20 min, the mixture was diluted with diethyl ether (300 mL) and the organic layer was separated. The aqueous layer was extracted with diethyl ether (3×100 mL), then the combined organic layers were washed with saturated aqueous $NaHCO_3$ (100 mL) and brine (100 mL), then dried and evaporated. The residue was directly used in the next demethylation step.

N-*Ethyl*-m-*methoxyaniline* (***6**-Me*): ^{1}H NMR (250 MHz, $CDCl_3$): δ = 1.26 (t, ^3J(H,H) = 7 Hz, 3H), 3.16 (q, ^3J(H,H) = 7 Hz, 2H), ≈3.5 (brs, 1H), 3.79 (s, 3H), 6.18 (t, ^4J(H,H) = 2 Hz, 1H), 6.27 (m, 2H), 7.10 ppm (t, ^3J(H,H) = 8 Hz, 1H); ^{13}C NMR (75.5 MHz, $CDCl_3$): δ = 14.8, 38.4, 55.0, 99.4 (CH), 104.0 (CH), 106.0 (CH), 130.2 (CH), 147.6 (C), 160.8 ppm (C).

N-*(2,2,2-Trifluoroethyl)*-m-*methoxyaniline* (***6**-CF$_3$)*:[29] ^{1}H NMR (250 MHz, $CDCl_3$): δ = 3.76/3.77 (2×t, ^3J(H,F) = 7 Hz), 3.78 (s, Σ 5H), 3.97 (brt, ^4J(H,F) = 6.0 Hz, 1H, NH), 6.24 (t, ^4J(H,H) = 2.3 Hz, 1H), 6.30 (dd, ^3J(H,H) = 8 Hz, ^4J(H,H) = 2 Hz, 1H), 6.37 (dd, ^3J(H,H) = 7.8 Hz, ^4J(H,H) = 2.4 Hz, 1H), 7.12 ppm (t, ^3J(H,H) = 7.8 Hz, 1H). ^{13}C NMR (62.9 MHz, $CDCl_3$): δ = 45.9 (q, ^2J(C,F) = 33 Hz), 55.1, 99.4 (CH), 104.0 (CH), 106.0 (CH), 125.0 (q, ^1J(C,F) = 280 Hz), 130.2 (CH), 147.6 (C), 160.8 ppm (C); EI-MS: *m/z*: 205 (80) $[M]^+$, 136 (100) $[M-CF_3]^+$.

N-*Ethyl*-N-*(2,2,2-trifluoroethyl)*-m-*methoxyaniline* (***8**)*: B.p. 87 °C (2.3 mbar); ^{1}H NMR (300 MHz, $CDCl_3$): δ = 1.19 (t, ^3J(H,H) = 7 Hz, 3H), 3.47 (q, ^3J(H,H) = 7 Hz, 2H), 3.80 (s, 3H), 3.83 (q, ^3J(H,F) = 8.9 Hz, Σ 5H), 6.36 (t, ^4J(H,H) = 1.5 Hz, 1H), 6.38–6.43 (m, 2H), 7.17 ppm (t, ^3J(H,H) = 8.1 Hz, 1H). ^{13}C NMR (62.9 MHz, $CDCl_3$): δ = 11.4 (Me), 45.6 (CH_2), 52.3 (q, ^2J(C,F) = 26 Hz), 55.1, 99.9 (CH), 102.5 (C), 105.9 (CH), 125.5 (q, ^1J(C,F) = 282 Hz), 130.0 (CH), 148.7 (C), 160.8 ppm (C); elemental analysis calcd. (%) for $C_{11}H_{14}F_3NO$: C 56.65, H 6.32, N 5.74; found: C 57.03, H 6.32, N 5.74.

General method for the demethylation of amines 6-CF$_3$, 9, and 12; synthesis of amines 7-H, 7-Et, and 13, respectively:[30] The starting amine (8.6 mmol) was dissolved in glacial AcOH (5 mL), then 48 % aqueous HBr (6 mL) was added and the mixture was heated at reflux for 7 h under argon (TLC of the neutralized probe indicated full conversion of the starting amine). After cooling, the solution was carefully neutralized to about pH 5–6 with aqueous NaOH (30 %). The organic phase was separated and the aqueous phase was extracted with $CHCl_3$ (3×20 mL). The combined organic fractions were carefully washed with saturated aqueous $NaHCO_3$ (50 mL), dried, and evaporated. The residue was dissolved in a small amount of $CHCl_3$ and filtered through SiO_2 (25 g) to remove impurities with very high and very low R_f values (eluent $CHCl_3$/MeOH (50:1) or hexane/EtOAc (2:1); yields 59–80 %).

N-*(2,2,2-Trifluoroethyl)*-m-*hydroxyaniline* (***7**-H)*:[31] M.p. 38 °C; ^{1}H NMR (300 MHz, $CDCl_3$): δ = 3.67 (t, ^3J(H,F) = 9 Hz), ≈5 (brs, 1H, NH), 6.24 (t, ^4J(H,H) = 2.3 Hz, 1H), 6.27 (m, 2H), 7.05 ppm (t, ^3J(H,H) = 8.1 Hz, 1H); ^{13}C NMR (75.6 MHz, $CDCl_3$): δ = 45.3 (q, ^2J(C,F) = 26 Hz), 100.3 (CH), 106.0 (C), 106.1 (CH), 124.9 (q, ^1J(C,F) = 280 Hz), 130.5 (CH),

 © 2009 Wiley-VCH Verlag GmbH & Co. KGaA, Weinheim

147.9 (C), 156.5 ppm (C); ^{19}F NMR (282.4 MHz, [D$_6$]acetone): $\delta=-72.3$ ppm (t, ^3J(H,H)=8.3 Hz); EI MS: m/z: 191 (76) $[M]^{+\cdot}$, 122 (100) $[M-CF_3]^+$; HRMS: m/z calcd for $C_8H_8NOF_3$: 192.06307; found: 192.06306 [M+H]; elemental analysis calcd (%) for $C_8H_8F_3NO$: C 50.27, H 4.22, N 7.33; found: C 49.92, H 3.99, N 7.01.

N-*Ethyl*-N-*(2,2,2-trifluoroethyl)*-m-*hydroxyaniline* (**7**-*Et*): ^{1}H NMR (300 MHz, $CDCl_3$): $\delta=1.18$ (t, ^3J(H,H)=7 Hz, 3H), 3.45 (q, ^3J(H,H)=7 Hz, 2H), 3.81 (q, ^3J(H,F)=9.0 Hz, 2H), 5.39 (brs, 2H), 6.29 (ddd, ^3J(H,H)=10 Hz, ^4J(H,H)=2.3 Hz, ^5J(H,F)=0.7 Hz, 1H), 6.30 (m, 1H), 6.38 (dd, ^3J(H,H)=8.3 Hz, ^4J(H,H)=2.5 Hz, 1H), 7.17 ppm (t, ^3J(H,H)=8.1 Hz, 1H); ^{13}C NMR (75.5 MHz, $CDCl_3$): $\delta=11.0$ (Me), 45.5 (CH_2), 51.9 (q, ^2J(C,F)=33 Hz), 100.2 (CH), 104.9 (C), 105.8 (CH), 125.5 (q, ^1J(C,F)=282 Hz), 130.2 (CH), 148.9 (C), 156.2 ppm (C); ESI-MS (negative mode): m/z: 218 (100) $[M-H]^-$, 435 (79) $2[M-H]^-$, 652 (58) $3[M-H]^-$; HRMS: m/z calcd for $C_{10}H_{12}F_3NO$: 220.09438; found: 220.09436 [M+H].

7-Hydroxy-N,2,2,4-tetramethyl-1,2-dihydroquinoline (***13***): M.p. 108 °C; ^{1}H NMR (300 MHz, $CDCl_3$): $\delta=1.27$ (s, 6H), 1.93 (d, ^4J(H,H)=1.4 Hz, 3H), 2.73 (s, 3H), 5.14 (q, ^4J(H,H)=1.4 Hz, 1H), 6.05 (d, ^4J(H,H)=1.9 Hz, 1H), 6.09 (dd, ^3J(H,H)=8.1 Hz, ^4J(H,H)=2.4 Hz, 1H), 6.89 (d, ^4J(H,H)=8.1 Hz, 1H); ^{13}C NMR (75.5 MHz, $CDCl_3$): $\delta=18.6$ (Me), 27.1 (Me×2), 30.7 (Me), 56.3 (C), 98.5 (CH), 102.5 (CH), 116.9 (C), 124.2 (CH×2), 127.3 (CH), 127.8 (C), 156.4 ppm (C); ESI-MS (positive mode): m/z: 204 (100) $[M+H]^+$; HRMS: m/z calcd for $C_{13}H_{17}NO$: 204.13829; found: 204.13829 [M+H].

Compound 10-H: A mixture of powdered phthalic anhydride (1.23 g, 7.50 mmol) and aniline **7**-H (1.08 g, 5.65 mmol) were heated with stirring under Ar at 160–170 °C for 3 h. Then a second portion of **7**-H (0.862 g, 4.51 mmol) and H_3PO_4 (5 mL, 85%) were added and the heating was continued for another 3 h. After cooling to RT, MeOH (10 mL) and water (2 mL) were added, the solution was seeded with powdered **10**-H, and the mixture was stirred at RT overnight. The resultant red solid was collected on a glass filter and recrystallized from MeOH to give the title compound as a bright red solid (732 mg, 30%); HPLC area: 95%, t_R= 9.4 min, impurity with t_R=6.9 min (eluent: A/B 60:40–0:100 in 25 min, 254 nm). ^{1}H NMR (300 MHz, [D$_6$]acetone): $\delta=3.97$ (brs, 2H, NH), 4.37 (q, ^3J(H,F)=9.1 Hz, 4H), 7.23 (s, 6H (6.94 (s, 4H) and 7.11 (s, 2H) in [D$_6$]DMSO)), 7.50 (2×dd, ^3J(H,H)=7.4 Hz, ^4J(H,H)=1.5 Hz, 1H), 7.83 (2×t, ^3J(H,H)=7.4 Hz), 7.90 (2×t, ^3J(H,H)=7.4 Hz, Σ 2H), 8.32 ppm (2×dd, ^3J(H,H)=7.7 Hz, ^4J(H,H)=1.6 Hz, 1H); ^{13}C NMR (75.5 MHz, $(CD_3)_2SO$): $\delta=43.7$ (q, ^2J(C,F)=32 Hz), 97.9 (C4/5), 107.2 (C8a/8b), 109.9 (C1/8), 123.8 (CH), 124.3 (CH), 125.5 (q, ^1J(C,F)=281 Hz), 126.4 (C), 128.3 (C2/7), 129.7 (CH), 135.1 (CH), 149.6 (C3/6 or C4a/4b), 152.0 (C4a/4b or C3/6), 152.1 (C2′), 168.5 ppm (CO); ^{19}F NMR (282.4 MHz, [D$_6$]DMSO): $\delta=-70.1$ ppm (t, ^3J(H,F)=9.0 Hz); HRMS: m/z calcd for $C_{24}H_{16}N_2O_3F_6$: 495.11379; found: 495.11374 [M+H].

Compound 10-Et: The title was obtained as described above by using amine **7**-Et (3.4 g, 15.5 mmol) and phthalic anhydride (24 mmol) and heating at 160 °C for 3 h followed by heating with an additional portion of **7**-Et (3.5 g, 16 mmol) and H_3PO_4 (7.0 mL) at 160 °C for 3 h. The warm reaction mixture was poured into aqueous MeOH (300 mL, 1:1), Et_3N (5 mL) was added to the solution, and the precipitate was filtered off and dried in vacuo to give the title compound in the CF as a light pink solid (4.5 g, 51%); HPLC area: 100%, t_R=10.1 min (eluent: A/B 50:50–0:100 in 25 min, 254 nm). M.p. 101–102 °C; ^{1}H NMR (300 MHz, $CDCl_3$): $\delta=1.20$ (t, ^3J(H,H)=7.0 Hz, 6H), 3.50 (q, ^3J(H,H)=7.0 Hz, 4H), 3.86 (q, ^3J(H,F)=8.9 Hz, 4H), 6.44 (dd, ^3J(H,H)=8.9 Hz, ^4J(H,H)=2.6 Hz, 2H), 6.59–6.65 (m, 4H), 7.19 (d, ^3J(H,H)=7.6 Hz, 1H), 7.56–7.70 (m, 2H), 8.00 ppm (d, ^3J(H,H)=7.2 Hz, 1H); ^{13}C NMR (75.5 MHz, $CDCl_3$): $\delta=11.3$ (Me), 45.8 (CH_2), 52.0 (q, ^2J(C,F)=33 Hz), 84.0 (C), 99.5 (CH), 108.4 (C), 108.9 (CH), 124.0 (CH), 124.8 (CH), 125.3 (q, ^2J(C,F)=282 Hz), 127.3 (C), 129.0 (CH), 129.5(CH), 134.7 (CH), 149.0 (C), 152.8 (C), 152.9 (C), 169.6 ppm (CO); ^{19}F NMR (282.4 MHz, $CDCl_3$): $\delta=-70.3$ ppm (t, ^3J(H,F)=8.9 Hz); ESI-MS (positive mode): m/z: 551 (100) $[M+H]^+$; HRMS: m/z calcd for $C_{30}H_{29}N_3O_{10}S_2$: 551.17639; found: 551.17637 [M+H]; elemental analysis calcd (%) for $C_{28}H_{24}F_6N_2O_3$: C 61.09, H 4.39, N 5.09; found: C 60.80, H 4.53, N 4.93.

7-Methoxy-2,2,4-trimethyl-1,2-dihydroquinoline (11):[32,29] Ytterbium(III) triflate (2.5 g, 5 mmol), which was previously dried in vacuo (1 mbar) at 150 °C, was added to a solution of *m*-anisidine (7.4 g, 60 mmol) in acetone (300 mL). The mixture was stirred at RT for 4 h, then the acetone was evaporated in vacuo and the residue was dissolved in EtOAc (500 mL), washed with water (100 mL) and brine (100 mL), and dried. The residue was purified on SiO_2 (100 g; eluent hexane/EtOAc 8:1) to give an oil that crystallized into a colorless solid with (8.0 g, 66%). M.p. 68 °C.

7-Methoxy-N,2,2,4-tetramethyl-1,2-dihydroquinoline (12): Compound **11** (6.85 g, 33.7 mmol), Cs_2CO_3 (6.2 g, 19 mmol), and MeI (8 mL, 128 mmol) were added to DMF (18 mL) and vigorously stirred at 90 °C for 3 h. The solvent was evaporated in vacuo (1 mbar), and the residue was taken up in diethyl ether (200 mL) and water (100 mL). The aqueous layer was acidified neutralized with 1 M HCl and extracted with diethyl ether (100 mL). The combined organic fractions were washed with brine (100 mL) and dried. After evaporation of the solvent, the title compound was isolated by chromatography on SiO_2 (200 g; eluent hexane/EtOAc 12:1) to give a colorless oil (5.2 g, 71%).

Compound 14-H: A solution of compound **13** (1.82 g, 8.96 mmol) and phthalic anhydride (1.04 g, 7.03 mmol) in propionic acid (6 mL) was heated with *p*-toluene sulfonic acid monohydrate (120 mg) at 160 °C for 24 h under Ar. The solvent was evaporated in vacuo and the residue was dissolved in CH_2Cl_2 (150 mL). The organic solution was washed with saturated aqueous $NaHCO_3$ (50 mL) and aqueous H_2SO_4 (0.5 M, 50 mL) and dried. After evaporation of the solvent, the title compound was isolated by chromatography on SiO_2 (350 g; eluent CH_2Cl_2/MeOH 15:1→0:1) to give a dark blue foam (1.3 g, 56%); HPLC area: 99%, t_R= 21.1 min (eluent: A/B 60:40–0:100 in 25 min, 590 nm). ^{1}H NMR (300 MHz, $CDCl_3$): $\delta=1.27$ (s, 6H), 1.30 (s, 6H), 1.62 (s, 6H), 2.83 (s, 6H), 5.17 (s, 2H), 6.29 (s, 2H), 6.30 (s, 2H), 7.14 (dd, ^3J(H,H)=6.8 Hz, ^4J(H,H)=1 Hz, 1H), 7.57 (m_c, 2H), 8.02 ppm (dd, ^3J(H,H)=6.9 Hz, ^4J(H,H)=1.3 Hz, 1H); ^{13}C NMR (75.5 MHz, $CDCl_3$): $\delta=18.2$ (2×Me), 27.7 (Me), 28.3 (Me), 31.1 (2×Me), 56.9 (C), 96.9 (2×CH), 106.6 (C), 120.0 (C), 122.1 (2×CH), 124.5 (CH), 125.4 (CH), 126.7 (C), 129.2 (CH), 129.3 (2×CH), 134.0 (CH), 147.7 (C), 153.2 (C), 169.8 ppm (CO); ESI-MS (positive mode): m/z: 519 (100) $[M+H]^+$.

Compound 14-SO$_3$H:[33] Rhodamine **14**-H (1.0 g, 1.9 mmol) was dissolved at 0 °C in conc. H_2SO_4 (20 mL, 96%) and the resultant orange–red solution was stirred at RT overnight. Then the reaction mixture was carefully diluted with dioxane (50 mL) and diethyl ether (500 mL) and kept at 0 °C for 2 h, then the solvent was decanted from the dark blue precipitate. The solid was dissolved in cold water, and the title compound was isolated by RP chromatography on Polygoprep 60-50 C18 (100 g; eluent methanol/water 1:1). Lyophilization gave the title compound as a voluminous dark blue crystalline mass (1.03 g, 76%); HPLC area: 92%, t_R=13.7 min (eluent: A/B 80:20–50:50 in 25 min, 590 nm). ^{1}H NMR (300 MHz, CD_3OD): $\delta=1.49$ (s, 6H), 1.53 (s, 6H), 3.14 (s, 6H), 3.53 (A part of AB system), 3.80 (B part of AB system, J_{AB}=14 Hz, Σ 4H), 5.87 (s, 2H), 6.73 (s, 2H), 7.29 (s, 2H), 7.31 (dd, ^3J(H,H)=7 Hz, ^4J(H,H)=1.6 Hz, 1H), 7.60 (m_c, 2H), 8.06 ppm (dd, ^3J(H,H)=7 Hz, ^4J(H,H)=1.4 Hz, 1H); HRMS: m/z calcd for $C_{34}H_{34}N_2O_9S_2$: 679.17785; found: 679.17774 [M+H].

Compound 1g: Compound **14**-SO$_3$H (110 mg, 0.162 mmol) and 2-aminoethanol (120 mg, 1.97 mmol) were dissolved in dry DMF (1 mL), then HATU (100 mg, 0.262 mmol) was added, followed by Et_3N (0.1 mL, 0.7 mmol). The solution gradually decolorized. The mixture was kept at 40 °C overnight, then the DMF was removed in vacuo and the residue was dissolved in methanol/water (1:1, 2 mL) and applied onto a column with Polygoprep 60-50 C18 (50 g; eluent methanol/water mixture 1:1) to give **1g**·nH$_2$NCH$_2$CH$_2$OH (R_f ~0.5) as a colorless oil (180 mg); HPLC area: 97%, t_R=12.9 min (eluent: A/B 80:20–50:50 in 25 min, 590 or 254 nm). ^{1}H NMR (300 MHz, CD_3OD, CF): $\delta=1.29$ (s, 6H), 1.36 (s, 6H), 2.83 (s, 6H), 2.95 (m, $H_2NCH_2CH_2OH$), 3.17 (t, ^3J(H,H)=5.5 Hz, 2H), 3.44 (A part of AB system), 3.52 (B part of AB system, J_{AB}=14), 3.56 (t, ^3J(H,H)=5.5 Hz, 2H), 3.70 (m, $H_2NCH_2CH_2OH$), 5.55 (s, 2H), 6.29 (s, 2H), 6.53 (s, 2H), 7.02 (m, 1H), 7.49 (m_c, 2H), 7.85 (m, 1H); ESI-MS (positive mode): m/z: 722 (52) $[M+H]^+$, 844 (89) $[M+2H_2NCH_2CH_2OH+H]^+$, 1063.8 (88); ESI-MS (negative mode): m/z: 720 (100) $[M-H]^-$, 781 (40) $[M-H+H_2NCH_2CH_2OH]^-$. By using ion-exchange resin in the H^+ form, 180 mg of the colorless

 © 2009 Wiley-VCH Verlag GmbH & Co. KGaA, Weinheim

1g·*n*$H_2NCH_2CH_2OH$ were transformed into 99 mg of **15**-H-OF (85% yield), which was isolated as dark blue foam after lyophilisation. ^{1}H NMR (300 MHz, D_2O, OF): δ = 1.50 (s, 6H), 1.60 (s, 6H), 3.13 (s, 6H), 3.15 (t, ^3J(H,H) = 6.1 Hz, 2H), 3.27 (t, ^3J(H,H) = 6.1 Hz, 2H), 3.68 (A part of AB system), 3.86 (B part of AB system, J_{AB} = 14.5 Hz, Σ 4H), 5.98 (s, 2H), 6.68 (s, 2H), 7.07 (s, 2H), 7.62 (d, ^3J(H,H) = 7.2 Hz, 1H), 7.84 (m, 2H), 7.96 (m, 1H); ESI-MS (positive mode): *m/z*: 766 (10) $[M-H+2Na]^+$; ESI-MS (negative mode): *m/z*: 720 (100) $[M-H]^-$.

Compound 15-CONHS: Compound **15**-H-OF (11 mg, 43 μmol) was suspended in MeCN (0.5 mL) and CH_2Cl_2 (0.5 mL), then Et_3N was added (50 μL, 350 μmol), followed by di(*N*-succinimidyl)carbonate (11 mg, 43 μmol). The clear dark blue–violet solution was stirred at RT overnight and gradually became colorless. Analysis by using HPLC indicated that the conversion was only about 15%. Di(*N*-succinimidyl)carbonate (40 mg, 156 μmol) was added and the reaction mixture was heated at 50°C. After 2 h, HPLC analysis indicated that the reaction mixture contained 77% of a substance with t_R = 14.3 min, 7% of the starting material (t_R = 12.9 min), and 6% of an impurity with t_R = 9.2 min (eluent: A/B 80:20–50:50 in 25 min, 590 nm). The solvents were evaporated, then the residue was dissolved in water with trifluoroacetic acid (0.1% (v/v), 0.5 mL) and centrifuged. The title compound was isolated from the supernatant solution by using HPLC. The blue fluorescent eluent, which contained a substance with t_R = 14.3 min, was evaporated in vacuo (1 mbar) until the solution froze to remove MeCN. The solid icy residue was lyophilized and the title compound was isolated as voluminous dark blue foam. ^{1}H NMR (600 MHz, D_2O, OF): δ = 1.43 (s, 6H), 1.52 (s, 6H), 2.91 (s, 4H), 3.05 (s, 6H), 3.39 (t, ^3J(H,H) = 4.8 Hz, 2H), 3.65 (A part of AB system), 3.83 (B part of AB system, J_{AB} = 14.3), 3.99 (t, ^3J(H,H) = 5 Hz, 2H), 5.90 (s, 2H), 6.62 (s, 2H), 7.05 (s, 2H), 7.54 (d, ^3J(H,H) = 7.3 Hz, 1H), 7.76 (m, 2H), 7.87 ppm (m, 1H); ESI-MS (negative mode): *m/z*: 861 (100) $[M-H]^-$; HRMS: *m/z* calcd for $C_{41}H_{42}N_4O_{13}S_2$: 863.22626; found: 863.22594 [*M*+H].

Compound 17: The title compound was obtained from 8-hydroxyjulolidine **16** (1.18 g, 6.26 mmol) and perfluorophthalic anhydride (1.0 g, 4.54 mmol) in propionic acid (7 mL) with *p*-toluenesulfonic acid monohydrate (80 mg) under the conditions described for rhodamine **14**-H. The solvent was evaporated in vacuo and the residue was separated on Polygoprep 60-50 C18 (100 g; eluent methanol/water 1:1→9:1 with 0.1% v/v TFA) to give a shiny dark green solid (0.869 g, 49%). ^{1}H NMR (300 MHz, $CDCl_3$): δ = 1.88 (s, 6H), 1.94 (m_c, 3H), 2.05 (s, 3H), 2.64–2.87 (m, 3H), 2.95 (apparent t, ^3J(H,H) = 6.2 Hz, 3H), 3.43 (m, 6H), 6.99 ppm (s, 2H); ^{19}F NMR (282 MHz, $CDCl_3$): δ = −138.4 (ddd, *J* = 24, 13, and 3 Hz), −140.4 (ddd, *J* = 22, 13, and 2 Hz), −153.0 (ddd, *J* = 24, 20, and 3 Hz), −159.3 ppm (dt, *J* = 21 and 2 Hz); ESI-MS (positive mode): *m/z*: 585 (100) $[M+Na]^+$; HRMS: *m/z* calcd for $C_{32}H_{26}F_4N_2O_3$: 653.19523; found: 563.19540 [*M*+H].

General method for the amidation of rhodamines 10, 10-H, 14-H, and 17 with aromatic amine 18; preparation of the methyl esters 19b–f: Dry rhodamine **10**-H, **10**-Et, **14**-H, or **17** (2.5 mmol) was suspended in dry 1,2-dichloroethane (50 mL) and $POCl_3$ (2 mL, 21 mmol) was added, then the mixture was heated at reflux under Ar for 4 h. All volatile materials were evaporated in vacuo (1–1.5 mbar) into a trap that was cooled with dry ice, and the residue was flushed with argon. Dry acetonitrile (50 mL) was added to the flask, followed by amine **18** (2.7 mmol, 632 mg) and triethylamine (1 mL, 7 mmol). The reaction mixture was heated at 90°C (bath temp.) for 24 h, then the solvent was evaporated in vacuo. The residue was dissolved in $CHCl_3$ (100 mL) and the organic solution was washed with water, 1 M aqueous HCl, water, and saturated aqueous $NaHCO_3$ (100 mL each) and dried. After evaporation of the solvent, the residue was dissolved in the minimum amount of warm dichloromethane and purified on SiO_2 (50 g; eluent hexane/EtOAc 4:1→1:1→1:4 with 0.1% Et_3N) to give solutions of methyl esters **19b–f**, which moved on the silica gel as yellowish bands. Colorless spots of **19b–f** on TLC (UV detection at λ = 254 nm) turned red in several minutes when the dry plates were exposed to normal laboratory light and air. Evaporation of the solvents gave oils that crystallized on trituration with MeOH or aqueous MeOH.

*Compound **19b***: M.p. 128°C (decomp.); ^{1}H NMR (300 MHz, $CDCl_3$): δ = 3.71 (s, 3H), 3.73 (m, 4H), 4.15 (t, ^3J(H,H) = 7 Hz, 2H, NH), 4.34 (s, 2H), 6.30 (dd, ^3J(H,H) = 8.6 Hz, ^4J(H,H) = 2.5 Hz, 2H), 6.38 (d, ^4J(H,H) = 2.4 Hz, 2H), 6.61 (d, ^3J(H,H) = 8.6 Hz, 2H), 7.09 (m, 1H), 7.22 (m, 1H), 7.53 (m_c, 2H), 7.59 (m, 2H), 8.00 (m, 1H); ^{19}F NMR (282.4 MHz, $CDCl_3$): δ = −72.2 ppm (t, ^3J(H,F) = 8.7 Hz); HRMS: *m/z* calcd for $C_{35}H_{24}N_4O_6F_6$: 711.16728; found: 711.16743 [*M*+H]; elemental analysis calcd (%) for $C_{35}H_{24}F_6N_4O_6$: C 59.16, H 3.40, N 7.88; found: C 58.88, H 3.53, N 8.02.

*Compound **19c***: Decomposed with melting on rapid heating up to ≈170°C; ^{1}H NMR (300 MHz, [D_6]acetone): δ = 1.16 (t, ^3J(H,H) = 7 Hz, 6H), 3.53 (q, ^3J(H,H) = 7.1 Hz, 4H), 3.68 (s, 3H), 4.12 (q, ^3J(H,F) = 9.3 Hz, 2H, NH), 4.35 (s, 2H), 6.58 (dd, ^3J(H,H) = 8.7 Hz, ^4J(H,H) = 2.7 Hz, 2H), 6.62 (d, ^4J(H,H) = 2.5 Hz, 2H), 6.77 (d, ^3J(H,H) = 8.9 Hz, 2H), 7.09 (m, 1H), 7.57 (m, 3H), 7.66 (dd, ^3J(H,H) = 8.2 Hz, ^5J(H,H) = 0.6 Hz, 1H), 7.78 (dd, ^4J(H,H) = 1.9 Hz, ^5J(H,H) = 0.6 Hz, 1H), 7.96 ppm (m, 1H); ^{13}C NMR (125.7 MHz, [D_6]acetone): δ = 11.5 (Me), 39.3 (CH_2), 46.4 (CH_2N), 51.9 (q, ^2J(C,F) = 33 Hz), 52.8 (OMe), 67.8 (C), 100.6 (CH), 109.2 (C), 110.6 (CH), 119.9 (CH), 123.3 (CH), 123.4 (CH), 123.6 (CH), 126.9 (q, ^1J(C,F) = 281 Hz) 129.1 (CH), 129.7 (CH), 130.2 (CH), 133.5 (C), 134.9 (CH), 144.4 (C), 149.8 (C), 153.2 (C), 154.6 (C), 167.3 (CO), 167.0 (CO), 168.7 (CO), 168.8 ppm (CO); ESI-MS (positive mode): *m/z*: 767 (18) $[M+H]^+$, 789 (26) $[M+Na]^+$, 1555 (100) $2[M+Na]^+$, 1586.8 (56); ESI-MS (negative mode): *m/z*: 765 (39) $[M-H]^-$, 1577 (100) $[M+HCOO]^-$; elemental analysis calcd (%) for $C_{39}H_{32}F_6N_4O_6$·0.5 $CHCl_3$: C 57.41, H 3.96, N 6.78; found: C 57.86, H 3.70, N 6.77.

*Compound **19e***: M.p. 172°C (decomp.); ^{1}H NMR (300 MHz, [D_6]acetone): δ = 1.24 (s, 6H), 1.29 (s, 6H), 1.62 (d, ^4J(H,H) = 1.3 Hz, 6H), 2.83 (s, 6H), 3.68 (s, 3H), 4.35 (s, 2H), 5.23 (q, ^4J(H,H) = 1.3 Hz, 2H), 6.24 (s, 2H), 6.44 (s, 2H), 7.12 (m, 1H), 7.57 (m_c, 2H), 7.68 (m, 2H), 7.89 (dd, ^4J(H,H) = 1.6 Hz, ^5J(H,H) = 0.9 Hz, 1H), 7.96 ppm (m, 1H); ^{13}C NMR (125.7 MHz, [D_6]acetone): δ = 18.4 (Me), 27.6 (Me), 28.2 (Me), 31.3 (Me), 39.3 (CH_2N), 52.7 (OMe), 57.3 (C), 67.8 (C), 98.3 (2× CH), 100.6 (CH), 119.7 (CH), 119.7 (CH), 121.0 (C), 121.9 (2×CH), 124.1 (CH), 124.4 (CH), 124.5 (CH), 127.2 (C), 128.8 (C), 129.5 (CH), 129.7 (C), 130.2 (CH), 130.3 (CH), 133.4 (C), 134.7 (CH), 144.7 (C), 147.6 (C), 153.0 (C), 154.7 (C), 167.2 (CO), 167.4 (CO), 168.6 (CO), 168.7 ppm (CO); ESI-MS (positive mode): *m/z*: 735 (100) $[M+H]^+$; HRMS: *m/z* calcd for $C_{45}H_{42}N_4O_6$: 735.31771; found: 735.31788 [*M*+H].

*Compound **19f***: Decomp. >280°C; ^{1}H NMR (600 MHz, $CDCl_3$): δ = 1.86 (m_c, 4H), 1.97 (m_c, 4H), 2.53 (m_c, 4H), 2.81 (m_c, 4H), 3.12 (m, 8H), 3.72 (s, 3H), 4.34 (s, 2H), 6.22 (s, 2H), 7.29 (dd, ^3J(H,H) = 8.2 Hz, ^4J(H,H) = 1.9 Hz, 1H), 7.61 (d, ^3J(H,H) = 8.2 Hz, 1H), 7.66 ppm (d, ^4J(H,H) = 1.9 Hz, 1H); ^{13}C NMR (125.7 MHz, $CDCl_3$; due to low intensities, signals from the fluorinated carbons were not recorded): δ = 21.0 (CH_2), 21.2 (CH_2), 21.8 (CH_2), 27.2 (CH_2), 38.7 (CH_2N), 49.3 (CH_2N), 49.8 (CH_2N), 52.6 (OMe), 66.7 (C), 102.2 (C), 108.0 (C), 117.7 (C), 120.7 (CH), 122.9 (2×CH), 124.0 (CH), 128.8 (C), 130.1 (CH), 132.5 (C), 142.0 (C), 144.3 (C), 147.5 (C), 162.7 (CO), 166.7 (CO), 166.9 (CO), 167.9 ppm (CO); ESI-MS (positive mode): *m/z*: 779 (100) $[M+H]^+$; 801 (27) $[M+Na]^+$; 1557 (19) $2[M+H]^+$; 1557 (19) $2[M+H]^+$; 1579 (11) $2[M+Na]^+$; HRMS: *m/z* calcd for $C_{43}H_{34}F_4N_4O_6$: 779.24872; found: 779.24912 [*M*+H].

General procedure for the cleavage of methyl esters 19b–f to lithium salts 1b–f: Methyl esters **19b–f** (0.5 mmol) were dissolved or suspended in dry EtOAc (7 mL), then LiI (260 mg, 1.94 mmol) was added and the mixture was heated in a closed glass thick-wall tube for 48 h (bath temp. 90°C). After cooling to RT, the precipitated LiOAc was removed by filtration and washed with EtOAc (2×1 mL), then dry diethyl ether (50 mL) was added slowly to the filtrate (concentrated in vacuo to about half of its volume) with stirring. Precipitated lithium salts **1b–f** were collected on a filter, washed with dry diethyl ether, and dried in vacuo. If THF was used as a solvent, the complete conversion took 4 d (and no AcOLi formed; it was not necessary to filter the reaction mixture before precipitating the corresponding lithium salts with diethyl ether).

*Compound **1b***: The title compound was obtained as a yellow–brown powder after heating a mixture of **19b** (35 mg) and LiI (26 mg) in EtOAc (1 mL) for 20 h (24 mg, 69%). ^{1}H NMR (300 MHz, CD_3OD): δ = 3.79 (q, ^3J(H,F) = 9.3 Hz, 4H), 4.09 (s, 2H), 6.40 (dd, ^3J(H,H) = 7.4 Hz, ^4J(H,H) =

 © 2009 Wiley-VCH Verlag GmbH & Co. KGaA, Weinheim

2.1 Hz, 2H), 6.41 (d, ^4J(H,H) = 1.9 Hz, 2H), 6.57 (d, ^3J(H,H) = 9.1 Hz, 2H), 7.11 (m, 1H), 7.18 (dd, ^3J(H,H) = 8.1 Hz, ^4J(H,H) = 1.9 Hz, 1H), 7.42 (dd, ^4J(H,H) = 1.8 Hz, ^5J(H,H) = 0.5 Hz, 2H), 7.59 (m, 3H), 7.98 ppm (ddd, ^3J(H,H) = 6.1 Hz, ^4J(H,H) = 1.3 Hz, ^5J(H,H) = 0.5 Hz, 1H); ^{13}C NMR (125.7 MHz, CD_3OD): δ = 42.1 (CH_2N), 45.8 (q, ^2J(C,F) = 33.5 Hz), 69.5 (C), 100.0 (2×CH), 108.9 (C), 111.3 (2×CH), 121.9 (CH), 124.3 (CH), 124.4 (CH), 125.0 (C), 125.2 (CH), ≈127 (q, ^1J(C,F) = 280 Hz), 128.7 (CH), 129.5 (2×CH), 130.0 (CH), 130.8 (C), 131.3 (C), 132.1 (CH), 134.4 (C), 135.3 (CH), 143.5 (C), 150.8 (C), 154.0 (C), 154.7 (C), 167.3 (CO), 168.8 (CO), 168.9 (CO), 169.8 (CO), 174.2 ppm (CO); ^{19}F NMR (282.4 MHz, $CDCl_3$): δ = −73.7 ppm (t, ^3J(H,F) = 9.0 Hz); ESI-MS (positive mode): *m/z*: 703 (100) $[M^-+H+Li]^+$; ESI-MS (negative mode): *m/z*: 695 (100) $[M]^-$. The carboxylic acid, which corresponds to lithium salt **1b**, was isolated in the OF by using HPLC (injection of a filtered solution of **1b** in MeCN/water (1:2), followed by gradient elution with the solvents and 0.1% TFA): t_R = 12.6 min (eluent: A/B 60:40–0:10 in 25 min, 254 nm).

Compound ***1c***: The title compound was isolated as a light brown powder after heating **19c** (816 mg) and LiI (584 mg) in THF (5 mL) for 4 d (702 mg, 87%; isolated as an oil that crystallized after triturating with diethyl ether). ^{1}H NMR (300 MHz, CD_3OD): δ = 1.14 (t, ^3J(H,H) = 7.1 Hz, 6H), δ = 3.47 (dq, ^5J(H,F) = 1.3 Hz, ^3J(H,H) = 7 Hz, 4H), 3.99 (q, ^3J(H,F) = 9.1 Hz, 4H), 4.1 (s, 2H), 6.51 (dd, ^3J(H,H) = 9 Hz, ^4J(H,H) = 2.5 Hz, 2H), 6.53 (d, ^4J(H,H) = 3 Hz, 2H), 6.65 (d, ^3J(H,H) = 8.7 Hz, 2H), 7.05 (m, 1H), 7.23 (dd, ^3J(H,H) = 8.1 Hz, ^4J(H,H) = 1.9 Hz, 1H), 7.44 (dd, ^4J(H,H) = 1.8 Hz, ^5J(H,H) = 0.5 Hz, 2H), 7.56 (m, 3H), 7.99 ppm (m, 1H); ^{13}C NMR (125.7 MHz, CD_3OD): δ = 11.7 (2×Me), 42.1 (CH_2N), 46.8 (2×CH_2N), 52.4 (q, ^2J(C,F) = 32.7 Hz), 69.1 (C), 100.8, 108.9 (2×), 110.7, 121.5, 124.3, 124.4, 125.1, 127.0 (q, ^1J(C,F) = 282 Hz), 129.5, 130.1, 130.5, 131.1, 131.8, 134.3, 135.3, 143.4, 150.2 (2×), 153.9 (2×), 154.5, 168.6 (CO), 168.8 (CO), 169.7 (CO), 174.2 ppm (CO); ^{19}F NMR (282.4 MHz, $CDCl_3$): δ = −73.7 ppm (t, ^3J(H,F) = 9.0 Hz); ESI-MS (positive mode): *m/z*: 797 (90) $[M^-+2Na]^+$, 1523 (100), 1539 (45); ESI-MS (negative mode): *m/z*: 751 (100) $[M]^-$, 1503 (82), 2[M^-+H] 1509 (100) 2-[M^-+Li].

Compound ***1d***: The preparation and properties of compound **1d** have been reported in reference [9].

Compound ***1e***: The title compound was isolated as a green powder after heating **19e** (117 mg) and LiI (56 mg) in EtOAc (1 mL) for 36 h (124 mg; the product contained ≈10% LiI that was very difficult to remove). ^{1}H NMR (300 MHz, CD_3OD): δ = 1.21 (s, 6H), 1.28 (s, 6H), 1.61 (d, ^4J(H,H) = 1.1 Hz, 6H), 2.76 (s, 6H), 4.1(s, 2H), 5.20 (q, ^4J(H,H) = 1.2 Hz, 2H), 6.16 (s, 2H), 6.32 (s, 2H), 7.04 (dd, ^3J(H,H) = 6.4 Hz, ^4J(H,H) = 1.5 Hz, 1H), 7.29 (dd, ^3J(H,H) = 8.1 Hz, ^4J(H,H) = 1.8 Hz, 1H), 7.45 (^4J(H,H) = 1.7 Hz, 1H), 7.54 (m, 3H), 7.98 ppm (dd, ^3J(H,H) = 6 Hz, ^5J(H,H) = 1.6 Hz, 1H); ^{13}C NMR (125.7 MHz, CD_3OD): δ = 18.4 (Me), 27.8 (Me), 28.2 (Me), 31.4 (Me), 42.1 (NCH_2), 57.8 (C), 69.9 (C), 98.6 (2×CH), 106.1 (2×C), 121.4 (CH), 121.5 (2×C), 122.2 (2×CH), 124.3 (CH), 124.4 (CH), 125.2 (CH), 127.6 (2×C), 130.0 (C), 130.6 (C), 130.8 (2×CH), 131.1 (C), 131.8 (CH), 134.4 (C), 135.3 (CH), 143.6 (C), 148.2 (C), 153.8 (C), 154.8 (C), 168.7 (CO), 168.8 (CO), 169.9 (CO), 174.2 ppm (CO); ESI-MS (positive mode): *m/z*: 749 (72) $[M^-+Li+Na]^+$, 765 (100) $[M^-+2Na]^+$; ESI-MS (negative mode): *m/z*: 751 (100) $[M]^-$. The carboxylic acid, which corresponds to lithium salt **1e**, was detected in the OF as a sharp peak in the HPLC (injection of a filtered solution of **1e** in MeCN/water (1:2), followed by gradient elution with the solvents and 0.1% TFA): t_R = 16.5 min (eluent: A/B 60:40–0:10 in 25 min, 254 nm).

Compound ***1f***: The title compound was isolated as a dark blue solid after heating **19f** (117 mg) of and LiI (48 mg) in boiling EtOAc (2 mL) for 36 h (95 mg). ^{1}H NMR (300 MHz, CD_3OD): δ = 1.88 (m_c, 4H), 1.98 (m_c, 4H), 2.58 (m_c, 4H), 2.78 (m_c, 4H), 3.12 (apparent q, ^3J(H,H) = 5.6 Hz, 8H), 4.1 (s, 2H), 6.39 (s, 2H), 7.23 (dd, ^3J(H,H) = 8.1 Hz, ^4J(H,H) = 1.8 Hz, 1H), 7.39 (d, ^4J(H,H) = 1.9 Hz, 1H), 7.62 (d, ^3J(H,H) = 8.1 Hz, 1H); ^{19}F NMR (282.4 MHz, CD_3OD): δ = −145.5 (dt, J = 19 and 6.7 Hz), −146.7 (dt, J = 18.8 and 3.3 Hz), −149.8 (dt, J = 18.5 and 6.8 Hz), −157.0 ppm (dt, J = 18 and 3.3 Hz); ESI-MS (positive mode): *m/z*: 765 (100) $[MH+H]^+$; ESI-MS (negative mode): *m/z*: 763 (100) $[M^-]$. The title lithium salt contained ≈9% of both dicarboxylic acids obtained in the course of opening of the phthalimide ring (δ = 3.85/3.86 (s, NCH_2), 6.74 (2×dd, J = 8 and 2 Hz), 7.00 (d, J = 2 Hz), 7.32 m, 7.40 ppm (d, J = 8 Hz)). The carboxylic acid, which corresponds to lithium salt **1f**, was purified in the OF by HPLC (injection of a filtered solution of **1f** in MeCN/water (1:2), followed by gradient elution with the solvents and 0.1% TFA): t_R = 18.6 min (eluent: A/B 70:30–0:10 in 25 min, 254 nm; t_R = 15.3/15.5 min for the impurities).

Acknowledgements

This work was supported by the Max-Planck-Gesellschaft, the Bundesministerium für Bildung und Forschug (BMBF) grant (Biophotonics III program), the European Union through a Marie Curie fellowship (to M.B.) and a project grant (to S.W.H.) within the NEST/Adventure program (SPOTLITE). The authors are very grateful to R. Machinek, Dr. H. Frauendorf, and their co-workers for recording numerous NMR and mass spectra in the Institut für Organische und Biomolekulare Chemie (Georg-August-Universität, Göttingen). The authors are grateful to Mr. J. Jethwa for critical reading of the manuscript and to Mr. H. Sebesse for his help in the preparation of Figure 6.

[1] E. Abbe, *Arch. Mikrosk. Anat. Entwicklungsmech.* **1873**, *9*, 413–420.

[2] For reviews, see: a) S. W. Hell, *Science* **2007**, *317*, 1749–1753; b) M. Heilemann, P. Dedecker, J. Hofkens, M. Sauer, *Laser Photonics Rev.* **2009**, *3*, 180–202; c) D. Evanko, *Nat. Methods* **2009**, *6*, 19–20; d) S. W. Hell, *Nat. Methods* **2009**, *6*, 24–32; e) J. Lippincott-Schwartz, S. Manley, *Nat. Methods* **2009**, *6*, 21–23; for recent reports, see: f) S. Van de Linde, U. Endesfelder, A. Mukherjee, M. Schüttpelz, G. Wiebusch, S. Wolter, M. Heilemann, M. Sauer, *Photochem. Photobiol. Sci.* **2009**, *8*, 465–469; g) V. Westphal, S. O. Rizzoli, M. A. Lauterbach, D. Kamin, R. Jahn, S. W. Hell, *Science* **2008**, *320*, 246–249; h) R. Schmidt, C. A. Wurm, S. Jakobs, J. Engelhardt, A. Egner, S. W. Hell, *Nat. Methods* **2008**, *5*, 539–544; i) B. Hein, K. I. Willig, S. W. Hell, *Proc. Natl. Acad. Sci. USA* **2008**, *105*, 14271–14276; j) M. Andresen, A. C. Stiel, J. Fölling, D. Wenzel, A. Schönle, A. Egner, C. Eggeling, S. W. Hell, S. Jakobs, *Nat. Biotechnology* **2008**, *26*, 1035–1040; k) S. E. Irvine, T. Staudt, E. Rittweger, J. Engelhardt, S. W. Hell, *Angew. Chem.* **2008**, *120*, 2725–2728; *Angew. Chem. Int. Ed.* **2008**, *47*, 2685–2688; l) M. C. Lang, T. Staudt, J. Engelhardt, S. W. Hell, *New J. Phys.* **2008**, *10*, 1–13; m) A. Punge, S. O. Rizzoli, R. Jahn, J. D. Wildanger, L. Meyer, A. Schönle, L. Kastrup, S. W. Hell, *Microsc. Res. Tech.* **2008**, *71*, 644–650; n) B. Harke, C. Ullal, J. Keller, S. W. Hell, *Nano Lett.* **2008**, *8*, 1309–1313; o) J. Fölling, S. Polyakova, V. Belov, A. van Blaaderen, M. L. Bossi, S. W. Hell, *Small* **2008**, *4*, 134–142.

[3] a) E. Betzig, G. H. Patterson, R. Sougrat, O. W. Lindwasser, S. Olenych, J. S. Bonifacino, M. W. Davidson, J. Lippincott-Schwartz, H. F. Hess, *Science* **2006**, *313*, 1642–1645; b) H. Shroff, C. G. Galbraith, H. White, J. Gilette, S. Olenych, M. W. Davidson, E. Betzig, *Proc. Natl. Acad. Sci. USA* **2007**, *104*, 20308–20313.

[4] a) M. J. Rust, M. Bates, X. Zhuang, *Nat. Methods* **2006**, *3*, 793–796; b) M. Bates, B. Huang, G. T. Dempsey, X. Zhuang, *Science* **2007**, *317*, 1749–1753; c) B. Huang, W. Wang, M. Bates, X. Zhuang, *Science* **2008**, *319*, 810–813; d) B. Huang, S. A. Jones, B. Brandenburg, X. Zhuang, *Nat. Methods* **2008**, *5*, 1047–1052.

[5] fPALM = fluorescent PALM: a) S. T. Hess, T. P. K. Girirajan, M. D. Mason, *Biophys. J.* **2006**, *91*, 4258–4272; b) M. F. Juette, T. J. Gould, M. D. Lessard, M. J. Mlodzianoski, B. S. Nagpure, B. T. Bennet, S. T. Hess, J. Bewersdorf, *Nat. Methods* **2008**, *5*, 527–529.

[6] W. E. Moerner, *Nat. Methods* **2006**, *3*, 781–782.

[7] K. H. Knauer, R. Gleiter, *Angew. Chem.* **1977**, *89*, 116–117; *Angew. Chem. Int. Ed. Engl.* **1977**, *16*, 113–113.

[8] H. Willwohl, J. Wolfrum, R. Gleiter, *Laser Chem.* **1989**, *10*, 63–72.

[9] J. Fölling, V. Belov, R. Kunetsky, R. Medda, A. Schönle, A. Egner, C. Eggeling, M. Bossi, S. W. Hell, *Angew. Chem.* **2007**, *119*, 6382–6386; *Angew. Chem. Int. Ed.* **2007**, *46*, 6266–6270.

 © 2009 Wiley-VCH Verlag GmbH & Co. KGaA, Weinheim

[10] A. Egner, C. Geisler, C. von Middendorf, H. Bock, D. Wenzel, R. Medda, R. Andresen, A. C. Stiel, S. Jakobs, C. Eggeling, A. Schönle, S. W. Hell, *Biophys. J.* **2007**, *93*, 3285–3290.
[11] J. Fölling, V. Belov, D. Riedel, A. Schönle, A. Egner, C. Eggeling, M. Bossi, S. W. Hell, *ChemPhysChem* **2008**, *9*, 321–326.
[12] H. Bock, C. Geisler, C. A. Wurm, C. von Middendorf, S. Jakobs, A. Schönle, A. Egner, S. W. Hell, C. Eggeling, *Appl. Phys. B* **2007**, *88*, 161–165 .
[13] a) M. Heilemann, E. Margeat, R. Kasper, M. Sauer, P. Tinnefeld, *J. Am. Chem. Soc.* **2005**, *127*, 3801–3806; b) J. Vogelsang, R. Kasper, C. Steinhauer, B. Person, M. Heilemann, M. Sauer, P. Tinnefeld, *Angew. Chem.* **2008**, *120*, 5545–5550; *Angew. Chem. Int. Ed.* **2008**, *47*, 5465–5469.
[14] A. Schönle, S. W. Hell, *Nat. Biotechnol.* **2007**, *25*, 1234–1235.
[15] M. Bossi, J. Fölling, V. N. Belov, V. P. Boyarskiy, R. Medda, A. Egner, C. Eggeling, A. Schönle, S. W. Hell, *Nano Lett.* **2008**, *8*, 2463–2468.
[16] Highly nucleophilic aliphatic amines react sluggishly on heating with methyl esters of rhodamines in aprotic solvents, and afford the corresponding CFs of the primary amides.
[17] Therefore, saponification of the methyl ester group in compounds **19b–f** by using aqueous NaOH is accompanied by ring-opening of the imide and formation of two regioisomeric 2-carboxybenzoylglycines.
[18] V. P. Boyarskiy, V. N. Belov, R. Medda, B. Hein, M. Bossi, S. W. Hell, *Chem. Eur. J.* **2008**, *14*, 1784–1792.
[19] Sulfonic acid residues may also result in a slight redshift of the long wavelength absorption band of **1a** (compared with the corresponding unsulfonated heterocycle).
[20] G. T. Hermanson, *Bioconjugate Techniques*, Academic Press, San Diego, **1996**, pp. 57–60.
[21] S. Bigotti, A. Volonterio, M. Zanda, *Synlett* **2008**, 958–962.
[22] For a method for the sulfonation of rhodamines, see: F. Mao, W.-Y. Leung, R. P. Haugland (Molecular Probes), US Patent 6130101, **2000**.
[23] The rigidized xanthene fragment in compounds **1a**,**e**, and **g** improves the conjugation between the lone electron pair of the nitrogen atom and the aromatic system and, therefore, decreases the basicity of the amino group.
[24] See reference [20], pp. 57–59.
[25] A. van Blaaderen, A. Vrij, *Langmuir* **1992**, *8*, 2921–2931.
[26] W. Denk, J. H. Strickler, W. W. Webb, *Science* **1990**, *248*, 73–76.
[27] J. Fölling, M. Bossi, H. Bock, R. Medda, C. A. Wurm, B. Hein, S. Jakobs, C. Eggeling, S. W. Hell, *Nat. Methods* **2008**, *5*, 943–945.
[28] J. Salazar, S. E. Lopez, O. Rebello, *J. Fluorine Chem.* **2003**, *124*, 111–113.
[29] For example, see: L. A. Robinson, M. E. Theoclitou, *Tetrahedron Lett.* **2002**, *43*, 3907–3910.
[30] R. Herrmann, H.-P. Josel, K.-H. Drexhage, J. Arden-Jacob (Boehringer Mannheim GmbH), US Patent 57550409, **1998**.
[31] E. R. Bissell, R. W. Swansiger, *J. Fluorine Chem.* **1978**, *12*, 293–306.
[32] For example, see: C. S. Yi, S. Y. Yun, *J. Am. Chem. Soc.* **2005**, *127*, 17000–17006.
[33] F. Mao, W.-Y. Leung, R.-P. Haugland, WO9915517, **1999**.

Received: May 19, 2009
Published online: September 16, 2009

 © 2009 Wiley-VCH Verlag GmbH & Co. KGaA, Weinheim